

RESEARCH ARTICLE

Transcription factor old astrocyte specifically induced substance is a novel regulator of kidney fibrosis

Ayaha Yamamoto¹ | Hitomi Morioki¹ | Takafumi Nakae¹ | Yoshiaki Miyake¹ |
 Takeo Harada¹ | Shunsuke Noda¹ | Sayuri Mitsuoka¹ | Kotaro Matsumoto¹ |
 Masashi Tomimatsu¹ | Soshi Kanemoto² | Shota Tanaka¹ | Makiko Maeda³ |
 Simon J. Conway⁴ | Kazunori Imaizumi⁵ | Yasushi Fujio^{1,3,6} | Masanori Obana^{1,6,7}

¹Laboratory of Clinical Science and Biomedicine, Graduate School of Pharmaceutical Sciences, Osaka University, Suita, Osaka, Japan

²Department of Functional Anatomy and Neuroscience, Asahikawa Medical University, Asahikawa, Hokkaido, Japan

³Laboratory of Clinical Pharmacology and Therapeutics, Graduate School of Pharmaceutical Sciences, Osaka University, Suita, Osaka, Japan

⁴Herman B. Wells Center for Pediatric Research, Indiana University School of Medicine, Indianapolis, IN, USA

⁵Department of Biochemistry, Institute of Biomedical & Health Sciences, Hiroshima University, Hiroshima, Japan

⁶Integrated Frontier Research for Medical Science Division, Institute for Open and Transdisciplinary Research Initiatives (OTRI), Osaka University, Suita, Osaka, Japan

⁷Radioisotope Research Center, Institute for Radiation Sciences, Osaka University, Suita, Osaka, Japan

Correspondence

Masanori Obana, Laboratory of Clinical

Abstract

Prevention of kidney fibrosis is an essential requisite for effective therapy in preventing chronic kidney disease (CKD). Here, we identify Old astrocyte specifically induced substance (OASIS)/cAMP responsive element-binding protein 3-like 1 (CREB311), a CREB/ATF family transcription factor, as a candidate profibrotic gene that drives the final common pathological step along the fibrotic pathway in CKD. Although microarray data from diseased patient kidneys and fibrotic mouse model kidneys both exhibit *OASIS/Creb311* upregulation, the pathophysiological roles of OASIS in CKD remains unknown. Immunohistochemistry revealed that OASIS protein was overexpressed in human fibrotic kidney compared with normal kidney. Moreover, OASIS was upregulated in murine fibrotic kidneys, following unilateral ureteral obstruction (UUO), resulting in an increase in the number of OASIS-expressing pathological myofibroblasts. In vitro assays revealed exogenous TGF- β 1 increased OASIS expression coincident with fibroblast-to-myofibroblast transition and OASIS contributed to TGF- β 1-mediated myofibroblast migration and increased proliferation. Significantly, in vivo kidney fibrosis induced via UUO or ischemia/reperfusion injury was ameliorated by systemic genetic knockout of *OASIS*, accompanied by reduced myofibroblast proliferation. Microarrays revealed that the transmembrane glycoprotein Bone marrow stromal antigen 2 (Bst2) expression was reduced in *OASIS* knockout myofibroblasts. Interestingly, a systemic anti-Bst2 blocking antibody approach attenuated kidney fibrosis in normal mice but not in *OASIS*

Abbreviations: ATF, activating transcription factor; Bst2, bone marrow stromal antigen 2; CKD, chronic kidney disease; cKO, conditional knockout; Col, collagen; CRE, cAMP responsive element; CREB, cyclic AMP responsive element binding protein; CREB31, cAMP responsive element-binding protein 3-like; ECM, extracellular matrix; EMT, epithelial mesenchymal transition; ER, endoplasmic reticulum; ESKD, end-stage kidney disease; Fn1, fibronectin 1; FGFBP1, fibroblast growth factor binding protein 1; GDF-15, growth differentiation factor-15; GRP78, glucose-regulated protein 78; HK-2, human proximal tubule cells; I/R, ischemia reperfusion; MMP, matrix metalloproteinase; NRK49F cells, normal rat kidney fibroblast cell line; OASIS, old astrocyte specifically induced substance; pDCs, plasmacytoid dendritic cells; Pdpn, podoplanin; Postn, periostin; RAAS, rennin-angiotensin-aldosterone system; sCr, serum creatinine; Srebp-2, sterol regulatory element-binding protein 2; SIP, site-1 protease; S2P, site-2 protease; TGF- β 1, transforming growth factor beta 1; UUO, unilateral ureteral obstruction; α -SMA (Acta2), alpha smooth muscle actin (Actin Alpha 2, Smooth Muscle).

This is an open access article under the terms of the Creative Commons Attribution-NonCommercial License, which permits use, distribution and reproduction in any medium, provided the original work is properly cited and is not used for commercial purposes.

© 2020 The Authors. *The FASEB Journal* published by Wiley Periodicals LLC on behalf of Federation of American Societies for Experimental Biology

Science and Biomedicine, Graduate School of Pharmaceutical Sciences, Osaka University, 1-6 Yamada-oka, Suita, Osaka 565-0871, Japan.
 Email: obana@phs.osaka-u.ac.jp

Funding information

MEXT | Japan Society for the Promotion of Science (JSPS), Grant/Award Number: 18K15027, 18H02603 and 18K19545; HHS | National Institutes of Health (NIH), Grant/Award Number: R01 HL148165; Takeda Science Foundation; Japanese Association of Dialysis Physicians (JAPD); Japan Agency for Medical Research and Development (AMED), Grant/Award Number: JP20am0101084

knockout mice after UUU, signifying Bst2 functions downstream of OASIS. Finally, myofibroblast-restricted *OASIS* conditional knockouts resulted in resistance to kidney fibrosis. Taken together, *OASIS* in myofibroblasts promotes kidney fibrosis, at least in part, via increased Bst2 expression. Thus, we have identified and demonstrated that *OASIS* signaling is a novel regulator of kidney fibrosis.

KEYWORDS

chronic kidney disease, fibrosis, myofibroblast, transcription regulation

1 | INTRODUCTION

Ten percent of general population worldwide suffers from chronic kidney disease (CKD). Importantly, CKD is a risk factor not only for the development of end-stage kidney disease (ESKD) but also for the incidence of cardiovascular diseases.^{1,2} The prevalence of CKD and the rate of its associated deaths are increasing worldwide. Moreover, the cost of caring for ESKD patients has put pressure on health care budgets.³ Although the medicines blocking renin-angiotensin-aldosterone system (RAAS) has been used for the management of CKD, no significant impact on kidney outcome was observed. Thus, novel therapeutic strategies for CKD are urgently needed. Kidney fibrosis is a common final pathway for almost all kidney diseases⁴ and progressive kidney fibrosis is correlated with impaired function.⁵ Therefore, inhibiting kidney fibrosis could be a potential therapeutic approach to halt the progression of CKD.

Old astrocyte specifically induced substance (OASIS), also called cAMP responsive element-binding protein 3-like 1 (CREB3L1), is a transcription factor which belongs to the CREB/ATF family, such as ATF6, Luman (Creb3), BBF2H7 (Creb3L2), CREBH (Creb3L3), and CREB4 (Creb3L4).⁶⁻⁹ OASIS is cleaved by site-1 protease (S1P) and site-2 protease (S2P) when cells are exposed to endoplasmic reticulum (ER) stress, resulting in the release of the N-terminal domain, though it localizes to the ER membrane under normal conditions.¹⁰ Activated N-terminal domain of OASIS transcription factor is transported to the nucleus and therein regulates its target genes, including GRP78,¹¹ collagen1a1,¹² and FGF1,¹³ and so on. Several groups have shown that OASIS played an important role as a tumor suppressor.¹⁴⁻¹⁶ In our previous reports, OASIS modulated ER stress signaling in astrocytes⁶ and played important roles in protection of the large intestinal mucosa during colitis inflammation.¹⁷ We and others also reported that OASIS regulates bone

formation.^{12,18,19} However, the pathophysiological roles of *OASIS* in many tissues, especially the kidney, remain to be clarified.

To identify potential novel therapeutic targets for CKD, we focused on kidney fibrosis. In response to injury, kidney fibroblasts respond by exiting their quiescent state in both the renal interstitium and wrapped around peritubular capillaries to become activated via multiple cues and diverse signaling pathways. Depending on the signal, cells may detach from the capillaries and start to proliferate, migrate to the injury site, differentiate into highly contractile myofibroblasts and/or increase extracellular matrix (ECM) deposition and remodeling.²⁰ If the damage is repeated or persistent, or particularly severe, this often results in CKD, with organ fibrosis as a hallmark of this pathogenesis.

For this reason, we investigated the pathophysiological significance of *OASIS* in kidney fibrosis, especially focusing on myofibroblasts in our present study.

2 | METHODS

2.1 | Study approval

The analysis of human kidney tissue was approved by Clinical Research Ethics Review Committee in Graduate School of Pharmaceutical Science, Osaka University (approved number: Yakuso30-4). Care of all animals was in compliance with the Osaka University Animal Care Guidelines. All experimental procedures conformed to the Guide for the Care and Use of Laboratory Animals, Eighth Edition, updated by the US National Research Council Committee in 2011, and were approved by Animal Care and Use Committee in Graduate School of Pharmaceutical Sciences, Osaka University (approved number: Douyaku 28-14, R01-1). The mice were maintained on a 12 hours light/dark cycle

with constant temperature and humidity at the Animal Care Facility of Graduate School of Pharmaceutical Sciences, Osaka University. And, the mice were allowed ad libitum access to water and standard diet. At the endpoints of all experiments, the mice were sacrificed by exsanguination under isoflurane anesthesia. All efforts were made to minimize distress. The sample size and the time when the experiments were performed were determined referring to our preliminary studies and previous report.²¹

2.2 | Kidney fibrosis models

C57BL/6J mice (8-10 weeks of age, male) were purchased from Japan SLC. Mice were subjected to unilateral ureteral obstruction (UUO). Briefly, under isoflurane anesthesia, the ureter was dissected and tied at two places with 7-0 silk sutures, followed by cutting between two ligated points. As control, sham surgery was performed in the same way as UUO without tying and cutting the ureter.

Mice were intraperitoneally injected with folic acid (250 mg/kg) dissolved in 0.3 M sodium bicarbonate solution. At 2 weeks after the injection, the transcript expression of *OASIS/Creb3l1* in kidney was measured.

Ischemia reperfusion (I/R) injury was induced by 22-min clamp of the unilateral renal artery/vein with animal-experimental disposable clips (Natsume Seisakusho). The body temperatures were maintained at 37°C during the operation. At 3 weeks after the operation, the kidneys were perfused with PBS and harvested.

2.3 | OASIS knockout mice/myofibroblasts-restricted OASIS knockout mice

OASIS knockout (KO) mice were established in a previous report.¹² *OASIS* KO mice were compared with age- (8-12 weeks) and sex-matched wild-type (WT) mice.

The targeting vector with loxP flanked exon2 of the mouse *OASIS/Creb3l1* gene was constructed to generate *OASIS* floxed mice. *OASIS* floxed mice were crossed with transgenic mice expressing periostin (Postn)-Cre recombinase,²² and Postn-Cre/*OASIS*^{fllox/fllox} mutant (*OASIS* cKO) mice were produced. Postn-Cre/*OASIS*^{wild/wild} mice were used as a control.

2.4 | Anti-Bst2 antibody treatment

Anti-Bst2 antibody and control Rat IgGκ were purchased from Novus Biologicals (DDX0390P-100) and BioLegend (400432), respectively. C57BL/6J mice (8 weeks of age, male) or *OASIS* KO mice were subjected to UUO, followed by intraperitoneal treatment with 100 μg/body antibody at

Day 1. Seven days after UUO, kidney fibrosis was evaluated by Sirius Red staining, Masson's trichrome staining and hydroxyproline assay, described below.

2.5 | Hydroxyproline assay

Kidney (20 mg wet weight) was homogenized in buffer containing 0.1 mol/L of NaCl and 5 mmol/L of NaHCO₃, and centrifuged at 15 000 rpm for 5 minutes. After washing with the buffer five times, the sample was hydrolysed in 6 N HCl for 5 hours at 120°C, and filtered through a 0.45 μm filter (Millipore). Hydrolysed samples were vacuum-dried at 45°C (EZ-2 Plus Genevac, SP Scientific), and suspended in distilled water. The samples were oxidized using fresh chloramine T solution containing 61.5 mmol/L of chloramine T (Nacalai tesque), 0.104 mol/L of sodium citrate, 0.56 mol/L of sodium acetate, and 30.8% isopropanol. After incubation for 20 minutes at room temperature, Ehrlich's reagent containing 0.42 mol/L of p-dimethylaminobenzaldehyde, 11% perchloric acid, and 81% isopropanol was added, and the samples were incubated for 40 minutes at 65°C. Subsequently, absorbance of the samples was measured at 560 nm using a micro plate reader (SpectraMAX M5e, Molecular Devices).

2.6 | Measurement of serum creatinine

Serum creatinine (sCr) was measured with LabAssay Creatinine kit (FUJIFILM Wako Pure Chemical Corporation) according to manufacturer's protocol.

2.7 | Cell culture

NRK49F cells were obtained from RIKEN CELL BANK and cultured in Dulbecco's Modified Eagles Medium (DMEM); high glucose with L-Glutamine and sodium bicarbonate (Sigma-Aldrich) supplemented with 10% fetal bovine serum (FBS). NRK49F cells were treated with TGF-β1 (peprotech), tunicamycin (Sigma-Aldrich) or angiotensin II (Sigma-Aldrich) in culture medium without FBS.

2.8 | Lentivirus production and infection

shRNAs targeting *OASIS/Creb3l1*, or non-target shRNA (control) from MISSION TRC shRNA lentiviral library were purchased from Sigma-Aldrich (*OASIS* #1: TRCN0000086318, #2: TRCN0000086320). Lentivirus particles were produced by co-transfection with 5.2 μg pNHP, 2.1 μg pVSV-G, 0.5 μg pCEP4-tat, and 2.6 μg shRNAs targeting *OASIS/Creb3l1* or control into 293T cells

using 60 μg polyethylenimine (Polyethylenimine “Max,” Polysciences, FL, USA). Cell culture media of 293T cells were changed to DMEM containing GlutaMAXTM with serum at 9-14 hours after the transfection. After 36 hours, culture supernatant containing lentivirus was filtered through a 0.45 μm filter. The supernatant was centrifuged at 23 000 rpm for 2 hours and the pellet was suspended with 100 μL of PBS. To knock down the expression of *OASIS/Creb3l1* in NRK49F cells, cells were incubated with DMEM containing a lentivirus vector at 2000-3000 MOI, 5 $\mu\text{g}/\text{mL}$ of Polybrene and serum for 24 hours.

Lentivirus expressing the full-length and N-terminal fragment of *OASIS/Creb3l1* were produced using similar methods, described above. Lentivirus expressing venus was used as a control. Each lentivirus was transfected into NRK49F cells for 24 hours.

2.9 | Scratch assay

NRK49F cells were seeded into a 24-well tissue culture plate. After 5 hours, Cells were transfected with *OASIS/Creb3l1* shRNA lentivirus or control for 24 hours, then stimulated with or without TGF- β 1 (10 ng/mL) for a day. The monolayer was scratched with a new 200 μL of pipette tip across the center of the well. At 0, 3, 6, 9, and 12 hours after the scratching, photographs were taken. The gap distance was measured at three separate regions using Image-J software and averaged. Measurements were performed by a blinded examiner.

2.10 | Cell proliferation assay

NRK49F cells were transfected with *OASIS/Creb3l1* shRNA lentivirus or control, followed by stimulation with TGF- β 1 (10 ng/mL) as described above. Cell proliferation was evaluated using the CellTiter Blue assay kit (Promega, Madison, WI), according to the manufacturer's protocol. The fluorescence was measured with SpectraMAX M5e (Molecular Devices, Sunnyvale, CA). The assays were performed in quadruplicate.

2.11 | Isolation of murine kidney myofibroblasts

Murine kidney myofibroblasts were isolated from WT and *OASIS* KO mice at Day 7 after UUO, as previously described.^{23,24} Briefly, the murine kidney cortex was minced and digested with the buffer including protease 14 (0.02 mg/mL, Sigma-Aldrich) and Liberase Blenzyme (0.3 mg/mL, Roche) for 2 hours. After filtration with 70 μm mesh and centrifugation, the cell suspension seeded in the culture dish for 4 hours

and then the nonadherent cells were removed. We confirmed that approximately 90% of adherent cells were α -SMA(+) myofibroblasts. The cells were cultured until 80% confluent. Based on our preliminary experiments, TGF- β signaling, which was induced by UUO surgery, was inactivated while myofibroblasts was cultured. Furthermore, to reduce the influence of various stimuli due to isolation of myofibroblasts from kidney and culture of myofibroblasts, and to find out the downstream molecule of *OASIS* specifically in TGF- β 1 signaling, cells were stimulated with TGF- β 1. Twenty-four hours after the stimulation, total RNA was prepared from the cells and microarray was performed, as described below.

2.12 | Human kidney tissue

Paraffin-embedded sections of human kidney tissues (sample diagnosis: Endstage kidney disease; #CS701402, #CS808093, Rejection of allograft of kidney; #CS803612, Within normal limits; #CS701403, #CS705934, #CS714584) were purchased from OriGene Technologies, Inc It was verified that fibrosis was observed in #CS701402, #CS808093 and #CS803612 samples. *OASIS* or α -SMA positive cells were stained by immunohistochemistry, as described below.

2.13 | Immunohistochemistry

Paraffin-embedded kidney sections were prepared at Day 7 after UUO. The sections were stained with anti-*OASIS* antibody (AF4080; R&D systems) by horseradish peroxidase detection system using Vectastain ABC kit (VECTOR LABORATORIES). The murine kidney sections were blocked with 3% BSA/TBS-0.1% TritonX-100 containing the kidney acetone powder from *OASIS* KO mice. The sections were also stained with anti- α -SMA antibody using alkaline phosphatase detection system. Nuclei were counter stained with hematoxylin. The number of *OASIS* positive nuclei was counted by a researcher who was blinded to the assay condition.

2.14 | Immunofluorescent microscopic analysis

Cells were fixed with 4% formaldehyde in PBS followed by blocking with 3% BSA for 1 hour. Thereafter, cells were stained with anti- α -SMA antibody or anti-*OASIS* antibody (AF4080; R&D). Alexa fluor546 anti-mouse IgG antibody was used as a secondary antibody.

Kidney sections were stained with anti- α -SMA and anti-Ki-67 (14-5698; eBioscience) antibodies. Alexa fluor546 anti-mouse IgG and Alexa fluor488 anti-Rat antibodies (Molecular Probes) were used as secondary antibodies.

α -SMA+ cells and Ki-67 + α -SMA+ cells were counted by the same researcher who was blinded to group assignment. Anti-Cre recombinase antibody was purchased from Chemicon (MAB3120).

Nuclei were identified by staining with DAPI. Stained cells and sections were evaluated by fluorescent microscopy (KEYENCE BZ-X700) or confocal fluorescence microscopy (Olympus FV3000).

2.15 | In situ hybridization

At Day 7 after UUO, kidney sections of WT or *OASIS* KO mice were digested with proteinase K, followed by fixation in 4% formaldehyde. Hybridization was carried out with *OASIS/Creb3l1* oligonucleotide probe labelled with digoxigenin (DIG) using DIG Oligonucleotide Tailing Kit, 2nd Generation (Roche) for 40 hours at 42°C. The oligonucleotide sequence for *OASIS/Creb3l1* antisense was 5'-CTCCACAAAGTGGTCCAGGTGCTCCGGGAAGTGCGCATTG-3'. After hybridization, the sections were incubated with anti-DIG-AP conjugate, Fab fragments (Roche), and then stained using alkaline phosphatase detection system.

2.16 | Histological analysis

Paraffin-embedded sections (3 μ m thick) from kidneys were prepared, and stained with the Sirius Red or Masson's trichrome. More than five fields in cortex were randomly selected from each mouse and the photomicrographs were taken. Sirius Red positive area was evaluated using Image J software by the same researcher who was blinded to group assignment.

2.17 | Reverse transcription/quantitative PCR

Total RNA was prepared from kidneys, as described previously.²⁵ First-strand cDNA was synthesized with the oligodeoxythymidine standard primer. PCR was performed using gene-specific primers. The PCR products were size-fractionated by 2% agarose gel electrophoresis. Quantitative PCR was performed using the Fast SYBR Green kit (Applied Biosystem, Waltham, MA, USA) to measure the expression of targeted gene. The primers used in this study are shown in Table S1.

2.18 | Immunoblot analysis

Immunoblot analysis was performed with anti-OASIS (MABE1017; Millipore), anti- α -SMA (A5228; SIGMA),

anti-GRP78 antibody (610978; BD biosciences) and anti-GAPDH (MAB374; Millipore) antibodies, as described previously.²⁵ For the detection of OASIS expression in kidneys, the membranes were blocked with 5% BSA/TBS-0.05% Tween-20 containing the kidney acetone powder from *OASIS* KO mice. Horseradish peroxidase (HRP)-conjugated antibody (Santa Cruz Biotechnology) was used as a secondary antibody. The bands were detected by ECL system (GE Healthcare) and densitometric analyses were performed using Image-J software.

2.19 | Chromatin immunoprecipitation assay

Myofibroblasts from murine kidney 7 days after UUO were isolated as described above, followed by TGF- β 1 treatment. Twenty-four hours after TGF- β 1 treatment, chromatin immunoprecipitation (ChIP) assay was performed with Simple ChIP Kit (Cell Signaling Technology) according to manufacturer's protocol. The primers used for ChIP assay are listed in Table S2.

2.20 | GeneChip analysis

Gene expression of primary murine kidney myofibroblasts was analyzed by a GeneChip system with Mouse Genome 2.0 ST Array (Affymetrix). Because the variance within *OASIS* KO myofibroblasts group was large, the threshold was set to >1.5 times and $P < .2$ to extract the genes which were changed by the deletion of *OASIS*.

2.21 | Statistics

All data are presented as means \pm SD. Comparisons were performed using student's *t* test or one-way analysis of variance (ANOVA) with post-hoc multiple comparison test. Differences were considered statistically significant when the calculated (two-tailed) *P*-value was $<.05$.

3 | RESULTS

3.1 | OASIS expression was upregulated in human CKD and murine fibrotic kidneys

To discover if OASIS is of relevance to human kidney diseases, we took advantage of the publicly available database Nephroseq. We found *OASIS/Creb3l1* mRNA levels were higher in kidneys of CKD patients compared with healthy controls (Figure S1A). Additionally, the expression of *OASIS/Creb3l1* transcript had a tendency to be enhanced as the severity of tubular atrophy and interstitial fibrosis

increased, though not statistically significant (Figure S1B). Immunohistochemical staining verified that, although the expression of OASIS was broadly detected in cytoplasm of tubular epithelial cells in normal parts of human kidney which is consistent with the data from the database THE HUMAN PROTEIN ATLAS (data not shown), the intensity of OASIS expression was increased in injured tubular epithelial cells of fibrotic kidneys (Figure 1A). Significantly, in fibrotic kidney tissue, the number of OASIS-positive nuclei were apparently upregulated in the tubulointerstitium (Figure 1A,B). Moreover, microarray analysis using murine kidney at Day 7 after UUO, a well-established model of kidney fibrosis, revealed *OASIS/Creb311* expression was upregulated roughly two-fold in murine fibrotic kidney (Table S3). Intriguingly, the expression of other members of the CREB/ATF family, including *Atf6*, *Creb3*, *Creb312*, *Creb313*, and *Creb314* did

not change after UUO. In addition, the expression level of *Sterol regulatory element-binding protein 2 (Srebp-2)*, which is cleaved by S1P as well as Atf6 and OASIS, was also unchanged between UUO and control group. To further evaluate the spatiotemporal expression of OASIS during fibrosis progression, C57BL/6J mice were subjected to UUO injury (Figure 2A-D). Quantitative PCR revealed *OASIS/Creb311* mRNA was upregulated at 3 days after UUO. Similarly, the protein level of the active form, but not full-length OASIS was also increased in a time-dependent manner after UUO. Seven days after UUO operation, the expression of α -SMA, a known myofibroblast marker, was detected. Furthermore, increased expression of *OASIS/Creb311* and *Acta2* (α -SMA) mRNA was also observed in kidneys at 2 weeks after folic acid-induced renal injury exhibiting interstitial fibrosis and at 3 weeks after I/R injury (Figure 2E-H). These data indicate

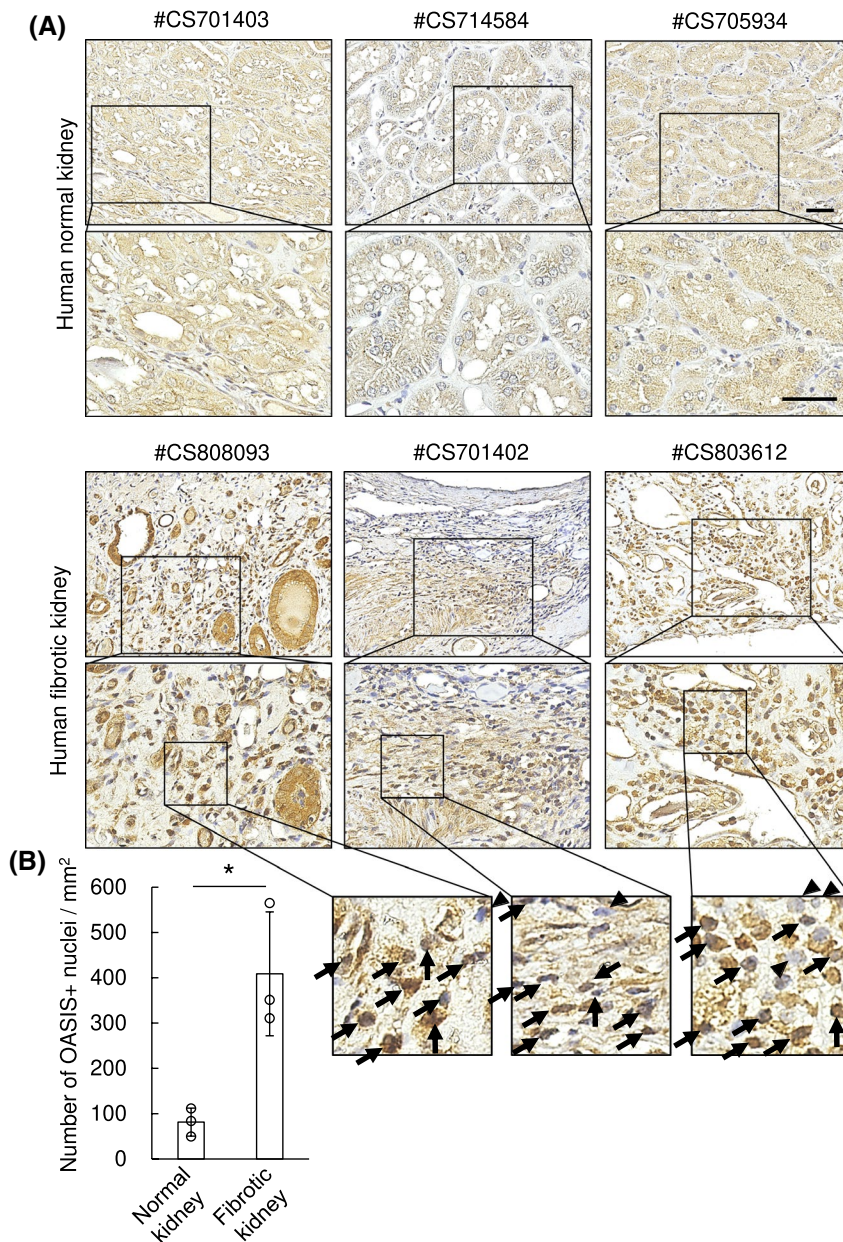


FIGURE 1 The number of OASIS-positive nuclei was increased in the tubulointerstitium area of human fibrotic kidneys. A, Immunohistochemical analysis was performed with anti-OASIS antibody (brown) in human kidney sections. Nuclei (blue) were stained with hematoxylin. Bar: 50 μ m. B, OASIS-positive nuclei were counted. Data are shown as mean \pm SD (n = 3) **P* < .05 by student's *t* test

that OASIS upregulation is associated with the progression of kidney fibrosis.

3.2 | The number of OASIS-expressing myofibroblasts was increased in the tubulointerstitium after UUO

To identify the cellular regions expressing OASIS in the kidney after UUO, we initially used in situ hybridization analysis which revealed *OASIS/Creb311* mRNA was mainly distributed in the tubulointerstitium and dilated tubules at Day 7 after UUO (Figure 3A). Moreover, immunohistochemical staining using an avidin-biotin-peroxidase and alkaline phosphatase detection system to identify OASIS and α -SMA myofibroblast marker,

confirmed OASIS was expressed in the tubulointerstitium, the perivascular region and the glomeruli in control contralateral kidney (but α -SMA was absent as uninjured). However, in the obstructed fibrotic kidney, the intensity of OASIS expression was increased in tubular epithelial cells broadly. Intriguingly, there is a significant increase in the number of OASIS/ α -SMA double-positive cells, and remarkably ~90% of α -SMA(+) myofibroblasts were stained by anti-OASIS antibody (Figure 3B,C). Similarly, OASIS and α -SMA double-positive cells were also detected in human fibrotic kidney (Figure S2), suggesting that OASIS-positive myofibroblasts contribute to the pathology of kidney fibrosis. Since the intensity and the amount of OASIS expression was higher in myofibroblasts than in the tubules of UUO kidneys, we focused on the role of OASIS in myofibroblasts in further experiments.

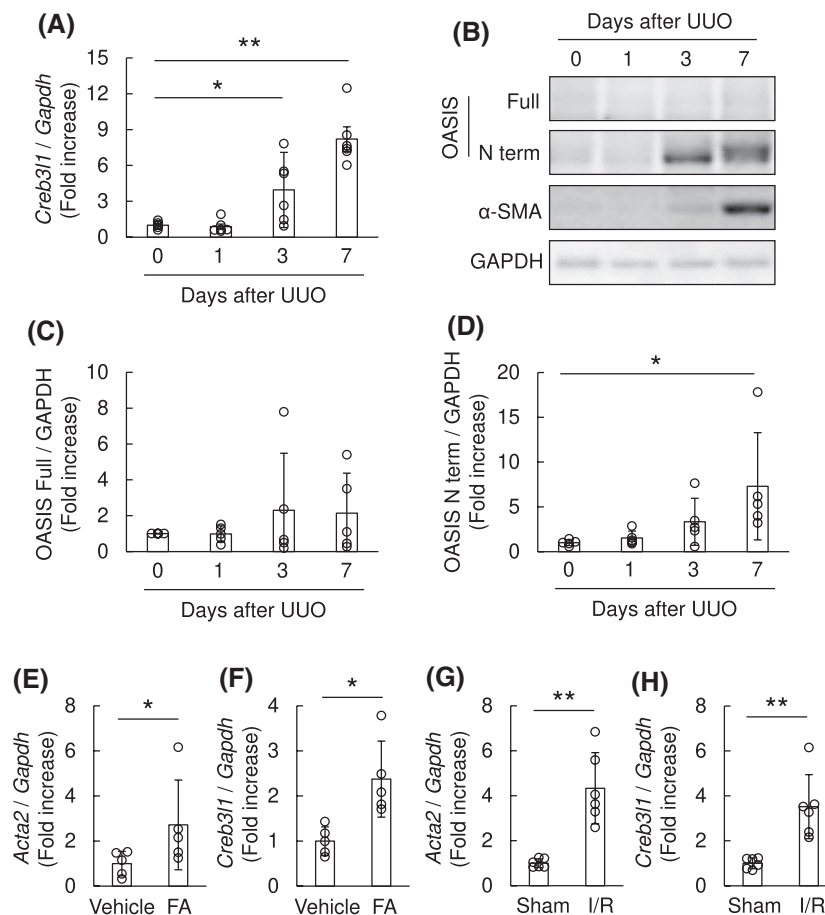


FIGURE 2 Expression of OASIS was upregulated in murine fibrotic kidneys. A, Total RNA was prepared from the murine kidneys after UUO. The expression of *OASIS/Creb311* transcript was analyzed at indicated time points after UUO by quantitative RT-PCR. The expression of the transcript was normalized to that of *Gapdh*. Data are shown as mean \pm SD (n = 6), ***P* < .01 vs. Day 0 by one-way ANOVA followed by Dunnett test. B, The kidney lysates from mice at 0, 1, 3 and 7 days after UUO were immunoblotted with anti-OASIS, anti- α -SMA and anti-GAPDH antibodies. Representative images are shown. C and D, Quantitative analysis for protein expression levels of OASIS in kidneys after UUO. Data are shown as mean \pm SD (n = 5), **P* < .05 vs. Day 0 by one-way ANOVA followed by Dunnett test. E-H, The expression of *Acta2* (E, G) and *OASIS/Creb311* (F, H) transcripts was estimated at 2 weeks after folic acid treatment (E, F; n = 5) or at 3 weeks after ischemia and reperfusion (I/R) injury (G, H; n = 6). The expression of the transcripts was normalized to that of *Gapdh*. Data are shown as mean \pm SD, **P* < .05, ***P* < .01 vs. vehicle or sham by student's *t* test

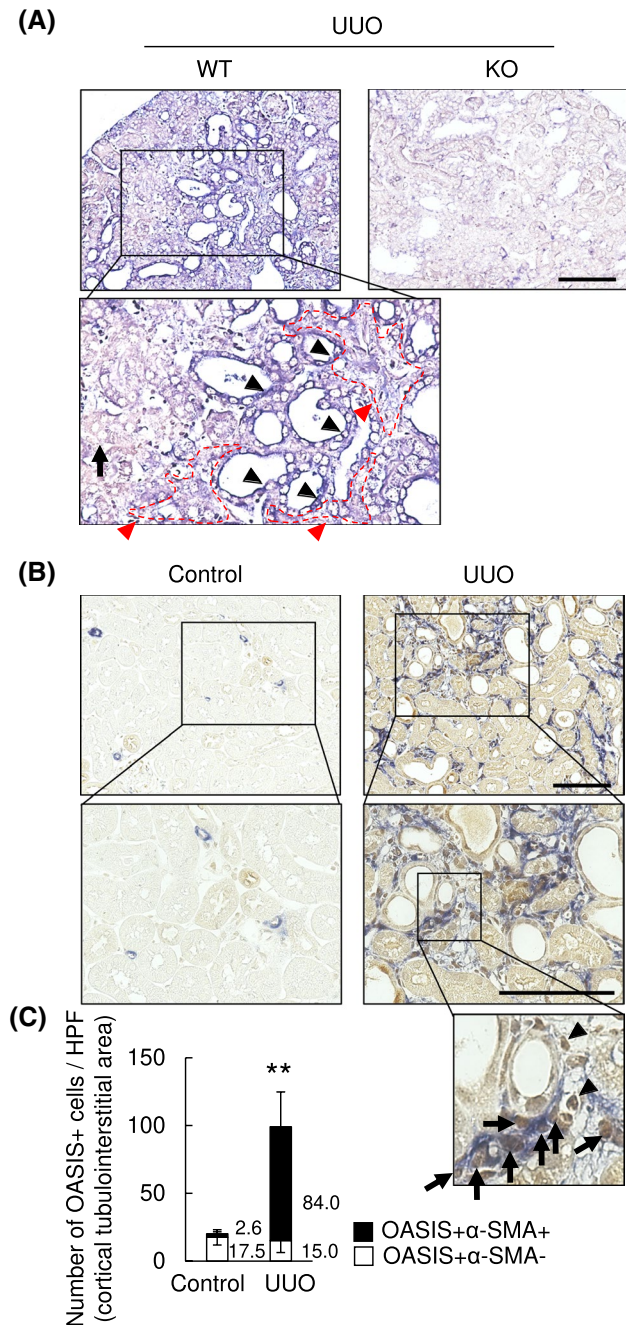


FIGURE 3 The number of OASIS positive myofibroblasts was significantly increased after UUO. Murine kidney sections were prepared 7 days after UUO. A, In situ hybridization analysis was performed. Black arrowheads: *OASIS/Creb311*-positive dilated tubules, black arrows: *OASIS/Creb311*-weakly positive/negative tubules, red arrows (the area surrounded by red dotted line): *OASIS/Creb311*-positive tubulointerstitial area, WT: Wild-type, KO: *OASIS* knockout mouse. Bar: 50 μ m. B, Immunohistochemical analysis was performed with anti-OASIS antibody (brown) and anti- α -SMA antibody (blue). Representative images are shown. Arrows: OASIS + α -SMA+ cells, arrowheads: OASIS + α -SMA- cells in the tubulointerstitium. Bar: 50 μ m. C, OASIS + cells in the tubulointerstitium were quantitatively estimated. Data are shown as mean \pm SD (n = 5 animals) ***P* < .01 by student's *t* test (Number of OASIS + α -SMA+ cells in contralateral (Control) kidney vs. OASIS + α -SMA+ cells in UUO kidney)

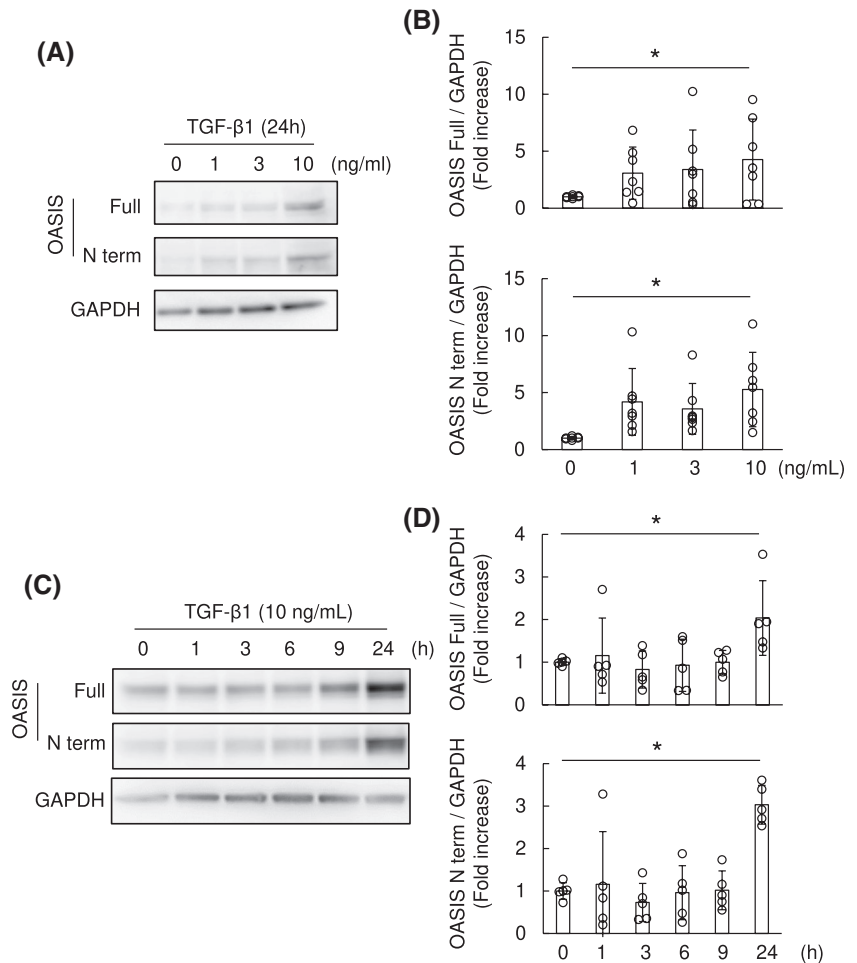
3.3 | TGF- β 1-induced OASIS expression in NRK49F cells

Resident fibroblasts in the tubular interstitium are thought to be the main source of myofibroblasts which contribute to the exacerbation of fibrosis in the injured kidney.²⁶ Thus, we focused on determining the functional roles of OASIS in fibroblasts/myofibroblasts, using NRK49F cells, cultured renal fibroblast cell line. Since previous studies showed that OASIS was activated by ER stress in osteoblasts and astrocytes,^{6,12} NRK49F cells were stimulated with tunicamycin, a powerful ER stress inducer (Figure S3A-C). Unexpectedly, although the known ER stress indicator GRP78 was induced by tunicamycin treatment in NRK49F cells, neither the full-length nor active form of OASIS was upregulated. As TGF- β was able to activate OASIS in human lung carcinoma cells,²⁷ NRK49F cells were treated with TGF- β 1, a well-known profibrotic cytokine (Figure 4A-D). Significantly, TGF- β 1 induced both the full-length and active form of OASIS expression in both a dose- and time-dependent manner. Consistent with this cumulative evidence, we confirmed that α -SMA expression was induced by TGF- β 1, as shown in Figure 5A,B. Moreover, since Angiotensin II can induce the differentiation of fibroblasts into myofibroblasts^{28,29} and there is cross-talk between the TGF- β 1 and Angiotensin II pathways,³⁰ NRK49F cells were treated with Angiotensin II (Figure S3D-F). However, Angiotensin II failed to increase the expression of OASIS, indicating that OASIS responds directly to pro-fibrotic TGF- β 1 stimulation and the acquisition of the properties of myofibroblasts did not involve OASIS expression.

3.4 | OASIS was necessary for the TGF- β 1-mediated migration and proliferation in myofibroblasts

To begin to determine the biological roles of TGF- β 1-induced OASIS, NRK49F cells were transfected with lentivirus expressing *OASIS/Creb311* shRNA or a scramble control, followed by TGF- β 1 stimulation. Although there was no difference in TGF- β 1-induced α -SMA expression between *OASIS* knockdown and control cells (Figure 5A,B) in vitro, quantitative PCR revealed whilst the expression of *Fibronectin* was unaltered, TGF- β 1-induced *Colla1* levels were suppressed in *OASIS* knockdown cells (Figure 5C,D). Therefore, it is conceivable that fibronectin was not directly regulated in NRK 49F cells by OASIS. Moreover, as was the case with osteoblasts,¹² chromatin immunoprecipitation revealed that OASIS directly bound the upstream site of *Colla1* gene in kidney myofibroblasts (Figure S4). Combined, these data suggested that *OASIS* knockdown inhibits the normal myofibroblast phenotype but did not affect

FIGURE 4 TGF- β 1 increased OASIS expression in NRK49F cells. A and B, NRK49F cells were stimulated with TGF- β 1 at the indicated concentrations for 24 hours. Immunoblotting was performed with anti-OASIS and anti-GAPDH antibodies. Representative images and quantitative analysis are shown. Data are shown as mean \pm SD * P < .05 vs. Day 0 by ANOVA followed by Williams test, (n = 7). C and D, NRK49F cells were stimulated with TGF- β 1 (10 ng/mL) for the indicated time. The cell lysates were immunoblotted with anti-OASIS and anti-GAPDH antibodies. Representative images and quantitative results are shown. Data are shown as mean \pm SD * P < .05 vs. Day 0 by ANOVA followed by Williams test (n = 5)



the TGF- β 1-mediated differentiation of fibroblasts into myofibroblasts. Next, wound healing assay was performed to determine the effects of altered OASIS expression upon migration. Interestingly, shRNA knockdown of *OASIS/Creb3l1* almost completely suppressed TGF- β 1-mediated migration (migration distance at 12 hours after TGF- β 1 treatment: sh-control/TGF- β 1(-); $100.8 \pm 5.1 \mu\text{m}$, sh-control/TGF- β 1(+); $187.8 \pm 25.8 \mu\text{m}$, sh*OASIS*#1/TGF- β 1(-); $103.6 \pm 2.7 \mu\text{m}$, sh*OASIS*#1/TGF- β 1(+); $106.1 \pm 7.8 \mu\text{m}$, sh*OASIS*#2/TGF- β 1(-); $104.1 \pm 13.4 \mu\text{m}$, sh*OASIS*#2/TGF- β 1(+); $115.7 \pm 11.0 \mu\text{m}$) (Figure 5E,F). Unexpectedly, migration of NRK49F cells was also reduced by lentiviral overexpression of active form of *OASIS/Creb3l1* cDNA (Figure S5A-C). In addition, shRNA *OASIS/Creb3l1* knockdown resulted in a significant decrease of TGF- β 1-induced proliferation of NRK49F cells (cell viability: sh-control/TGF- β 1(-); $100.0 \pm 0.9\%$, sh-control/TGF- β 1(+); $139.3 \pm 1.7\%$, sh*OASIS*#1/TGF- β 1(-); $99.6 \pm 5.3\%$, sh*OASIS*#1/TGF- β 1(+); $120.5 \pm 4.2\%$, sh*OASIS*#2/TGF- β 1(-); $100.4 \pm 0.8\%$, sh*OASIS*#2/TGF- β 1(+); $114.8 \pm 1.4\%$) (Figure 5G). Since, unlike the migration, the degree of suppression of proliferation by *OASIS* knockdown was not complete, these data suggest that *OASIS* promotes migration of myofibroblasts, at least in part, independently of proliferation of myofibroblasts. Taken

together, *OASIS* was necessary for the TGF- β 1-mediated migration, proliferation, and collagen deposition of cultured myofibroblasts in vitro.

3.5 | Genetic deletion of *OASIS* ameliorated kidney fibrosis after UUO and I/R injuries

In order to assess the in vivo pathophysiological roles of *OASIS* in fibrotic kidney, we used *OASIS* KO mice.¹² *OASIS* KO mice and WT mice, as a control, were subjected to UUO. Using in situ hybridization (Figure 3A), PCR, immunoblotting and immunohistochemical staining (Figure S6), we confirmed that *OASIS* KO mice are nulls and lack *OASIS* mRNA and protein expression in kidneys. Interestingly, Sirius Red and Masson's trichrome staining demonstrated that interstitial fibrosis was reduced by 50% in *OASIS* KO mice compared with WT mice at Day 7 after UUO, though there was no histological difference in the contralateral kidneys between these two groups (Figure 6A,B). Consistent with histological analysis, hydroxyproline content was significantly reduced in *OASIS* KOs after UUO (WT-cont; $0.20 \pm 0.04 \mu\text{g}/\text{mg}$, WT-UUO; $0.48 \pm 0.08 \mu\text{g}/\text{mg}$, KO-cont; $0.19 \pm 0.04 \mu\text{g}/\text{mg}$, KO-UUO;

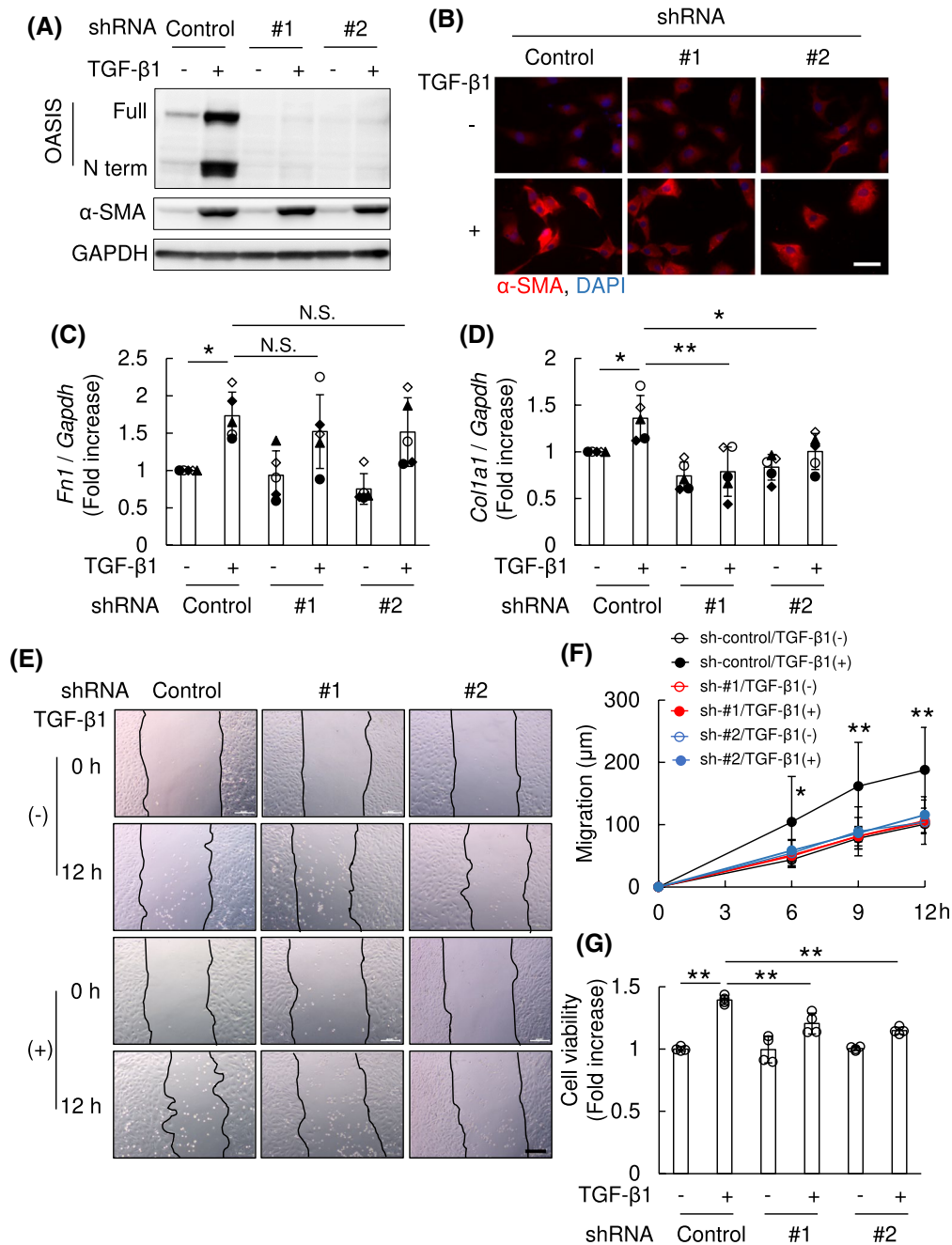


FIGURE 5 OASIS was necessary for TGF-β1-mediated migration and proliferation in NRK49F cells. NRK49F cells were transfected with lentivirus expressing shRNA against *OASIS/Creb311* (*OASIS*; #1 and #2), or a scramble control. At 24 hours after transfection, cells were stimulated with TGF-β1 (10 ng/mL) for 24 hours. A, Immunoblot analysis was performed using anti-OASIS, anti-α-SMA and anti-GAPDH antibodies. Representative images are shown. Experiments were repeated three times with similar results. B, Immunofluorescence analysis was performed with anti-α-SMA antibody. Nuclei were identified by DAPI. Representative images are shown. Bar: 50 μm. C and D, Quantitative PCR was performed for transcript expression of *fibronectin* (*Fn1*) and *collagen1a1* (*Col1a1*). The expression of the transcripts was normalized to that of *Gapdh*. Data are shown as mean ± SD (n = 5 times). The types of dot plots were displayed for each assay. *P < .05, **P < .01 by one-way ANOVA followed by Dunnett test. E and F, Cell migration induced by TGF-β1 was examined by scratch assay. Representative images are shown (E, Bar: 200 μm). The migration distance was measured (F). Data are shown as mean ± SD (n = 7) *P < .05, **P < .01 vs. other conditions by one-way ANOVA followed by Dunnett test. G, Cell proliferation was examined by CellTiter-Blue Cell viability assay. Values are shown as mean ± SD (quadruplicate), **P < .01 by one-way ANOVA followed by Dunnett test. Similar results were obtained from four independent experiments

0.37 ± 0.05 μg/mg) (Figure 6C). Moreover, the number of α-SMA positive myfibroblasts was also significantly decreased in *OASIS* KO mice (Figure 6D,E). To measure cell

proliferation index of myfibroblasts in vivo, kidney sections of *OASIS* KO mice and WT mice were co-stained with anti-Ki-67 and α-SMA antibodies. Consistent with in vitro

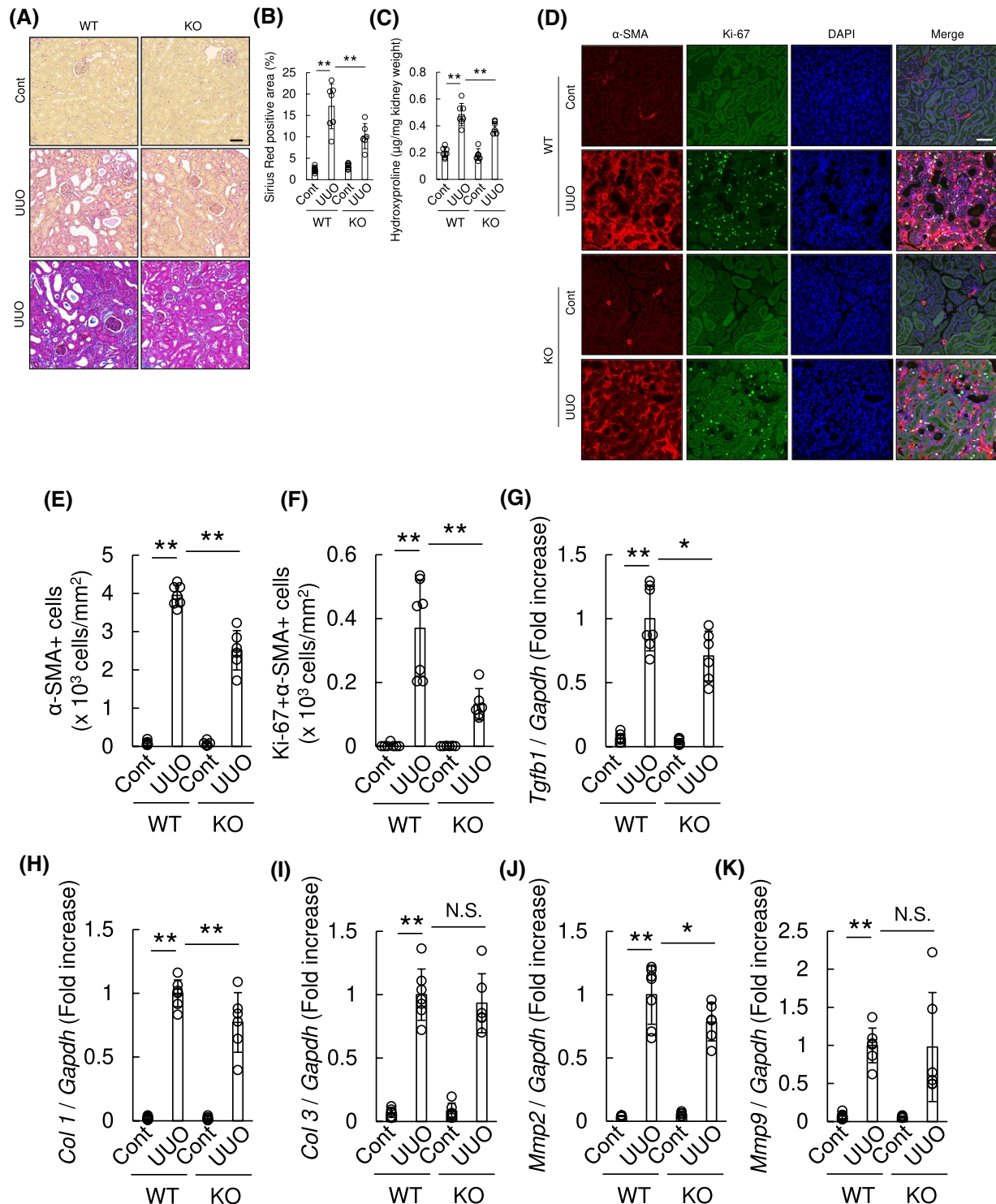


FIGURE 6 Kidney fibrosis was reduced in OASIS KO mice after UUO. WT and *OASIS* KO mice were exposed to UUO, and analyzed at 7 days after UUO. Contralateral kidney (Cont) was used as a control. A, Representative images show the results of Sirius Red staining (upper and middle panel) or Masson's trichrome staining (lower panel). Bar: 50 μ m. B, Sirius Red positive area was calculated. C, Hydroxyproline content in the kidney tissues was evaluated. D, Immunofluorescence analysis was performed with anti-Ki-67 antibody, anti- α -SMA antibody and DAPI. Representative images are shown. Bar: 50 μ m. E and F, The number of α -SMA+ cells (E) and the number of Ki-67 + α -SMA+ cells (F) was counted. G-K, Quantitative PCR was performed for transcript expression of *Tgfb1*, *Col 1*, *Col 3*, *Mmp2* and *Mmp9*. The expression of the transcripts was normalized to that of *Gapdh*. * $P < .05$, ** $P < .01$, by one-way ANOVA followed by Dunnett test. Data are shown as mean \pm SD (n = 7 for WT, n = 6 for KO)

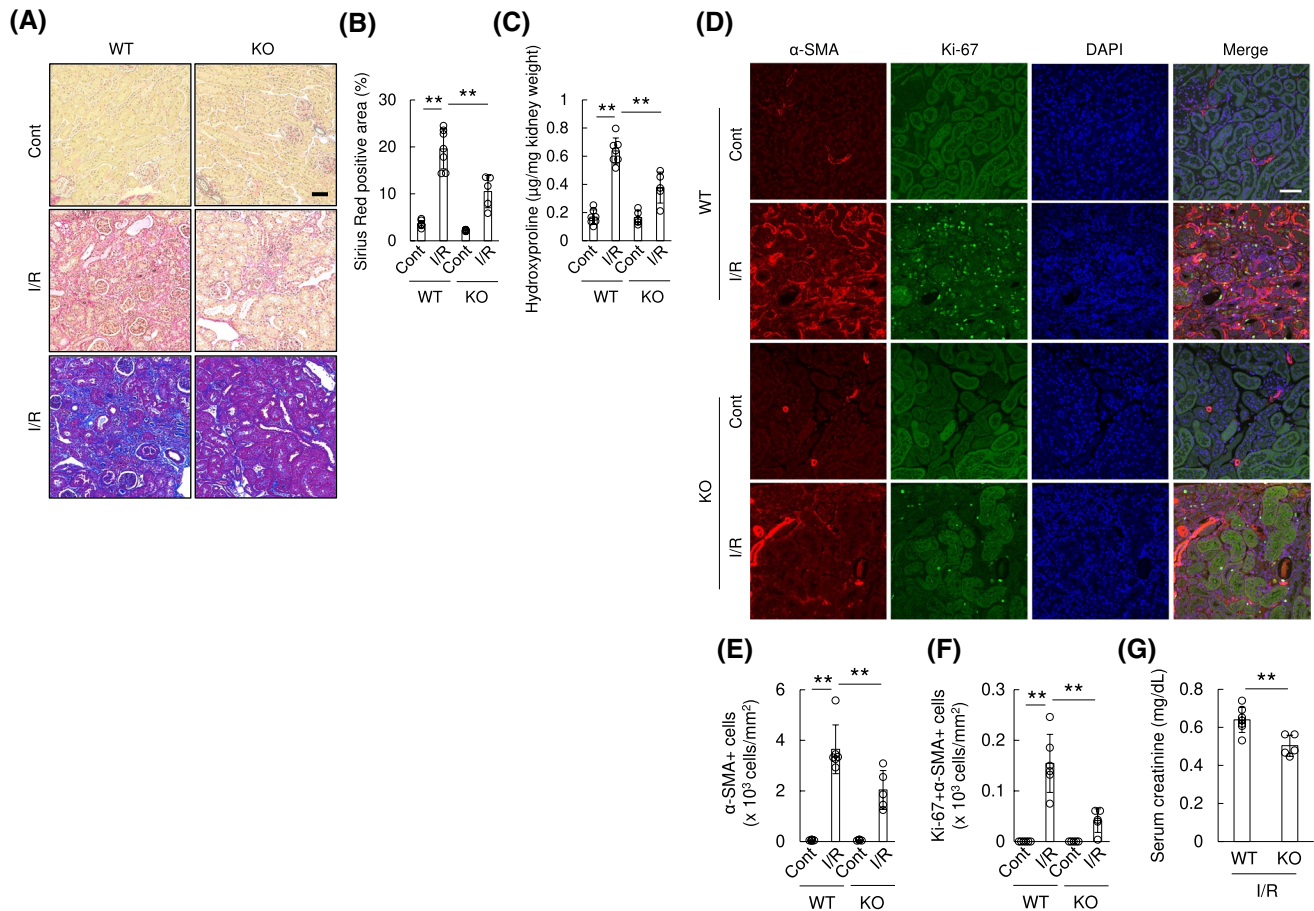


FIGURE 7 Genetic deletion of OASIS resulted in decreased kidney fibrosis after ischemia and reperfusion. WT and *OASIS* KO mice were subjected to unilateral renal I/R. A, Three weeks post I/R, the kidney sections were stained with Sirius Red (upper and middle panel) or Masson's trichrome (lower panel). Representative images are shown. Bar: 50 μ m. B, Sirius Red positive area was evaluated. C, Hydroxyproline content in the kidney tissues was evaluated. D, Immunofluorescence analysis was performed with anti-Ki-67 antibody, anti- α -SMA antibody, and DAPI. Representative images are shown. Bar: 50 μ m. E and F, The number of α -SMA+ cells (E) and the number of Ki-67 + α -SMA+ cells (F) was counted. ***P* < .01 by one-way ANOVA followed by Dunnett test. G, Serum creatinine level was measured 3 weeks after I/R. ***P* < .05 by student's *t* test. Data are shown as mean \pm SD (n = 6 for WT, n = 5 for KO)

findings (Figure 5G), the number of Ki-67/ α -SMA double-positive cells decreased in kidneys of *OASIS* KO mice after UO compared with WT mice (Figure 6D,F). Furthermore, quantitative PCR revealed that the mRNA level of outcome parameters of tissue fibrosis, such as *Tgfb1*, *Colla1*, and *Matrix metalloproteinase (MmpP) 2*, was significantly suppressed in *OASIS* KO mice after UO (Figure 6G-K). However, *OASIS* KO did not significantly influence the mRNA expression of *Col3* and *Mmp9* in kidney after UO probably because the standard deviation was large. To examine whether OASIS is also a driver of fibrosis in other forms of kidney diseases, I/R injury was induced in WT and *OASIS* KO mice. Concerning the effects of *OASIS* deletion on acute kidney injury, we confirmed that bilateral I/R-induced acute injury was not reduced in *OASIS* KO mice compared with WT mice, by analyzing serum creatinine level (data not shown). At chronic phase after unilateral I/R injury, progressive renal interstitial fibrosis was

significantly ameliorated in *OASIS* KO mice (Sirius Red positive area: WT; $19.6 \pm 4.2\%$, KO; $10.5 \pm 3.4\%$, hydroxyproline content: WT-cont; 0.15 ± 0.04 μ g/mg, WT-I/R; 0.61 ± 0.06 μ g/mg, KO-cont; 0.15 ± 0.04 μ g/mg, KO-I/R; 0.38 ± 0.13 μ g/mg) (Figure 7A-C). Similarly, proliferative myofibroblast numbers were reduced in *OASIS* KO mice compared with WT mice 3 weeks after I/R (Figure 7D-F). In this model, sCr level was increased in WT model 3 weeks after I/R injury (WT, sham; 0.32 ± 0.02 , 3 weeks; 0.64 ± 0.07 mg/dL), but the increase of sCr level by I/R injury was suppressed in *OASIS* KO mice compared with WT mice (Figure 7G) though there was no difference in sCr level at baseline between these mice (KO, sham; 0.35 ± 0.09 , 3 weeks; 0.50 ± 0.06 mg/dL), indicating that kidney function was preserved in *OASIS* KO mice in the chronic phase after I/R. These findings demonstrate that OASIS plays a pivotal role in the progression of fibrosis in kidney in response to different injuries.

3.6 | OASIS exerts its pro-fibrotic effects in part by regulating *Bst2* expression in fibrotic kidneys

To extend our understanding of the underlying mechanisms of OASIS-mediated pro-fibrotic effects other than collagen

synthesis (Figure 5D and Figure S4), primary myofibroblasts were isolated from kidneys of WT and *OASIS* KO mice at Day 7 after UUO and then were treated with TGF- β 1. Twenty-four hours after TGF- β 1 treatment, total mRNA was extracted from myofibroblasts and subjected to microarray analysis (Figure 8A). As a result, 72 annotated genes

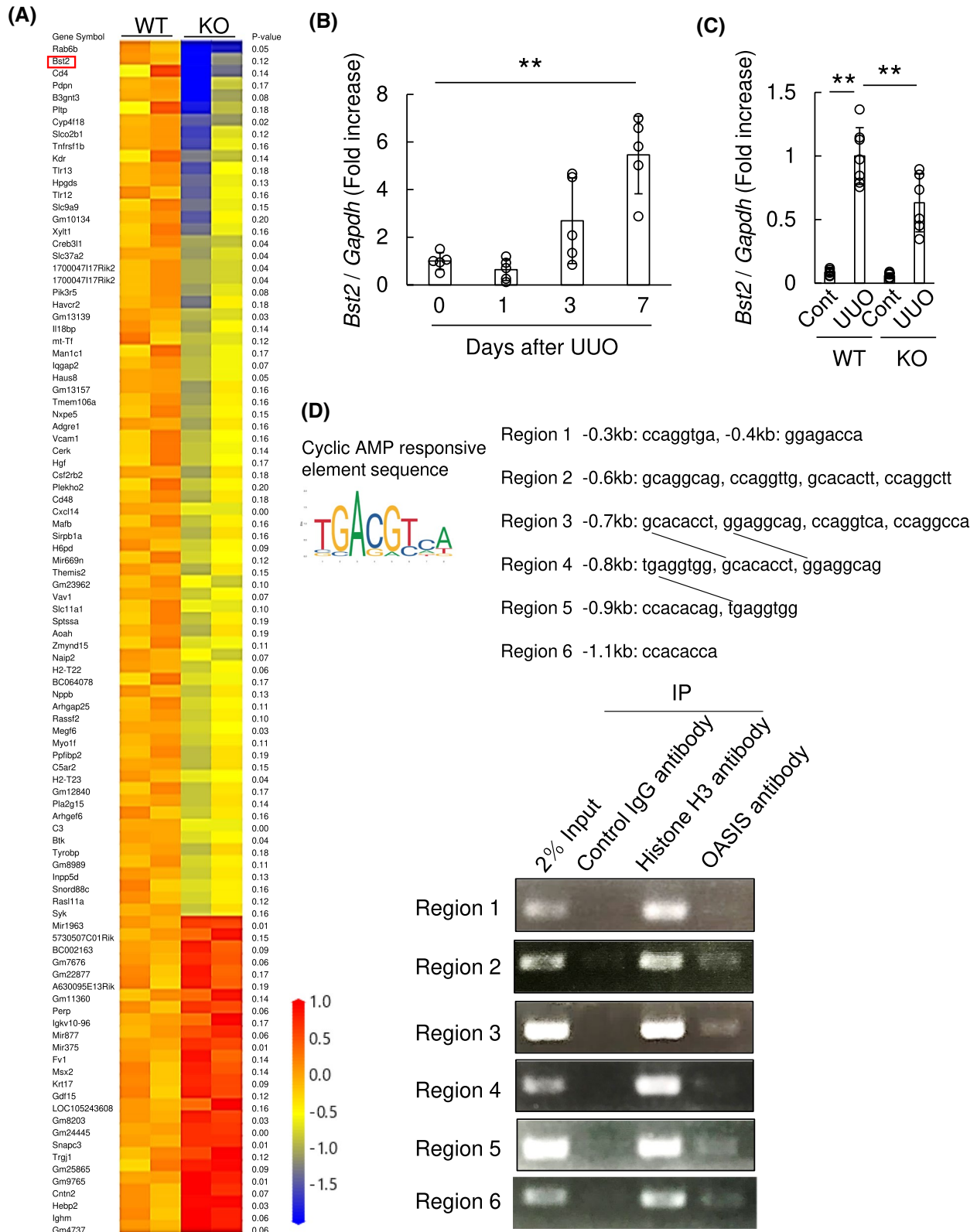


FIGURE 8 Blocking *Bst2*, a candidate downstream pro-fibrotic effector of OASIS, attenuated kidney fibrosis. A, Myofibroblasts were isolated from kidneys of WT and *OASIS* KO mice at Day 7 after UUO. Twenty-four hours after TGF- β 1 treatment, the total mRNA was extracted from the cells and microarray analysis was performed ($n = 2$ in each group). Heat map shows the genes with >1.5 -fold change between WT and *OASIS* KO cells with a P -value of <0.2 . B, The expression of *Bst2* transcript was measured at indicated time points after UUO by quantitative RT-PCR. The expression of the transcript was normalized to that of *Gapdh*. Data are shown as mean \pm SD ($n = 5$). C, At Day 7 after UUO, the transcript expression of *Bst2* in kidney of WT and *OASIS* KO mice was analyzed by quantitative PCR. Data are shown as mean \pm SD ($n = 7$ for WT, $n = 6$ for KO). D, Upper panel, cAMP responsive element-like sequence was cited from JASPAR and was picked up in the upstream region of *Bst2* gene. The line indicates same sequence. Lower panel, isolated myofibroblasts were treated with TGF- β 1 and chromatin immunoprecipitation assay was conducted. E-G, C57BL/6J mice were intraperitoneally treated with anti-*Bst2* antibody or control IgGk at Day 1 after UUO. E, Seven days after UUO, Sirius Red (upper and middle panel) or Masson's trichrome (lower panel) staining was performed. Representative images are shown. Bar: 50 μ m. F, Sirius Red positive area was measured. G, Hydroxyproline assay was performed. Data are shown as mean \pm SD ($n = 8$). H, *OASIS* KO or WT mice were intraperitoneally treated with anti-*Bst2* antibody or control IgGk at Day 1 after UUO. Hydroxyproline assay was performed at Day 7 after UUO. Data are shown as mean \pm SD ($n = 6$ for WT, $n = 5$ for KO). * $P < .05$, ** $P < .01$ by one-way ANOVA followed by Dunnett test

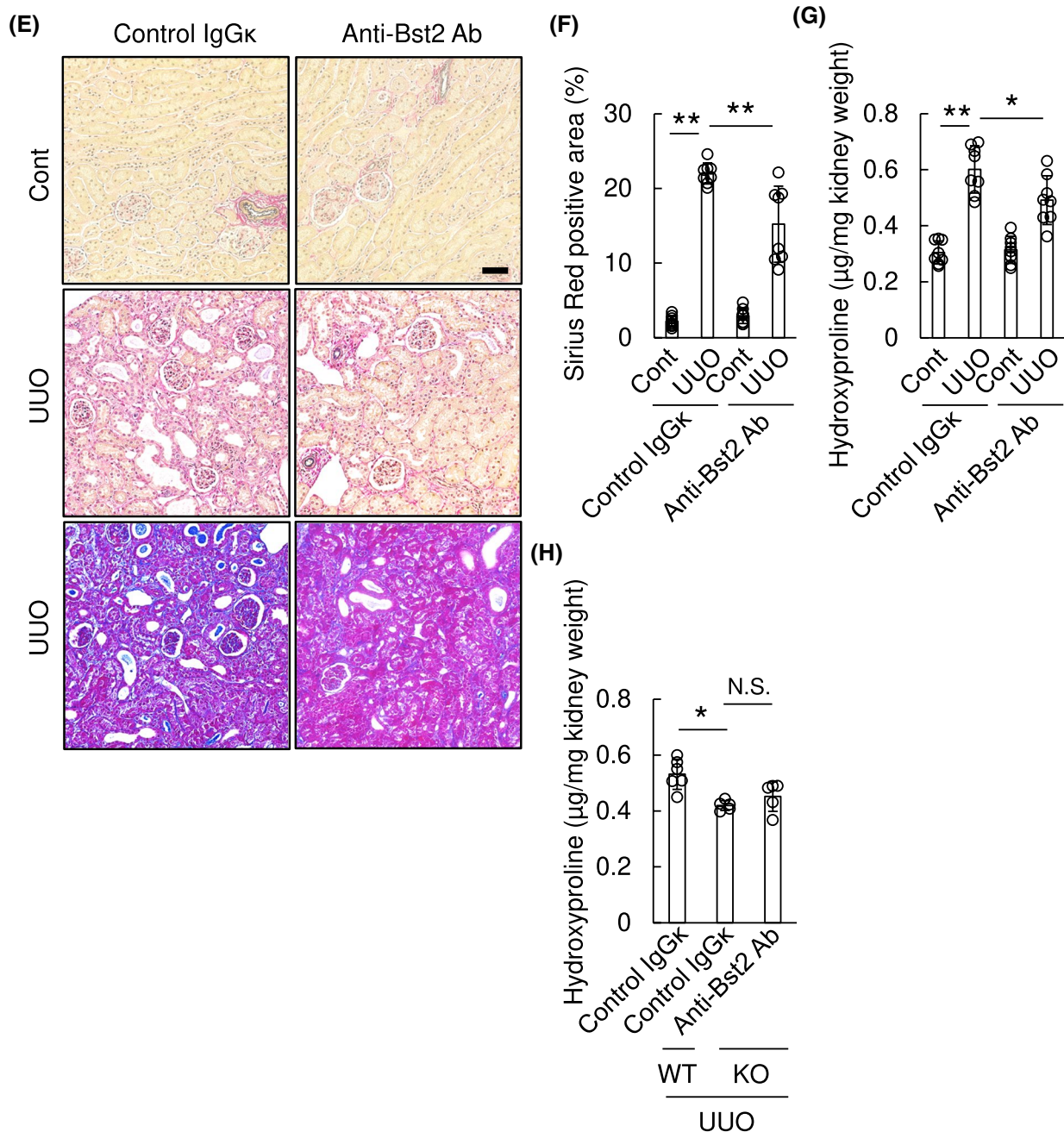


FIGURE 8 (Continued)

were decreased, whereas 26 annotated genes were increased in *OASIS* KO myofibroblasts using the criteria, described method section. Among these genes, *Bst2* (also termed CD317, HM1.24 or tetherin), a type II transmembrane glycoprotein, was significantly under-represented in *OASIS* KO myofibroblasts. Significantly, *Bst2* is thought to be responsible for proliferation and migration in cancer cells^{31,32} and was upregulated in kidneys of CKD patients (via Nephroseq database, Figure S7). Thus, we examined this candidate first. Fascinatingly, *Bst2* mRNA was upregulated after UUO with

similar kinetics to *OASIS/Creb311* (Figure 8B). In addition, quantitative PCR demonstrated that UUO-increased *Bst2* expression was significantly suppressed in kidneys of *OASIS* KO mice (Figure 8C). Furthermore, to test whether *OASIS* directly regulates *Bst2* expression, isolated myofibroblasts from murine kidneys were treated with TGF- β 1 and chromatin immunoprecipitation was conducted. As *OASIS* can bind to cAMP responsive element (CRE), we searched for CRE-like sequence in the upstream region of *Bst2* gene between 0 and 1.1kb, according to the previous report,^{33,34} and focused

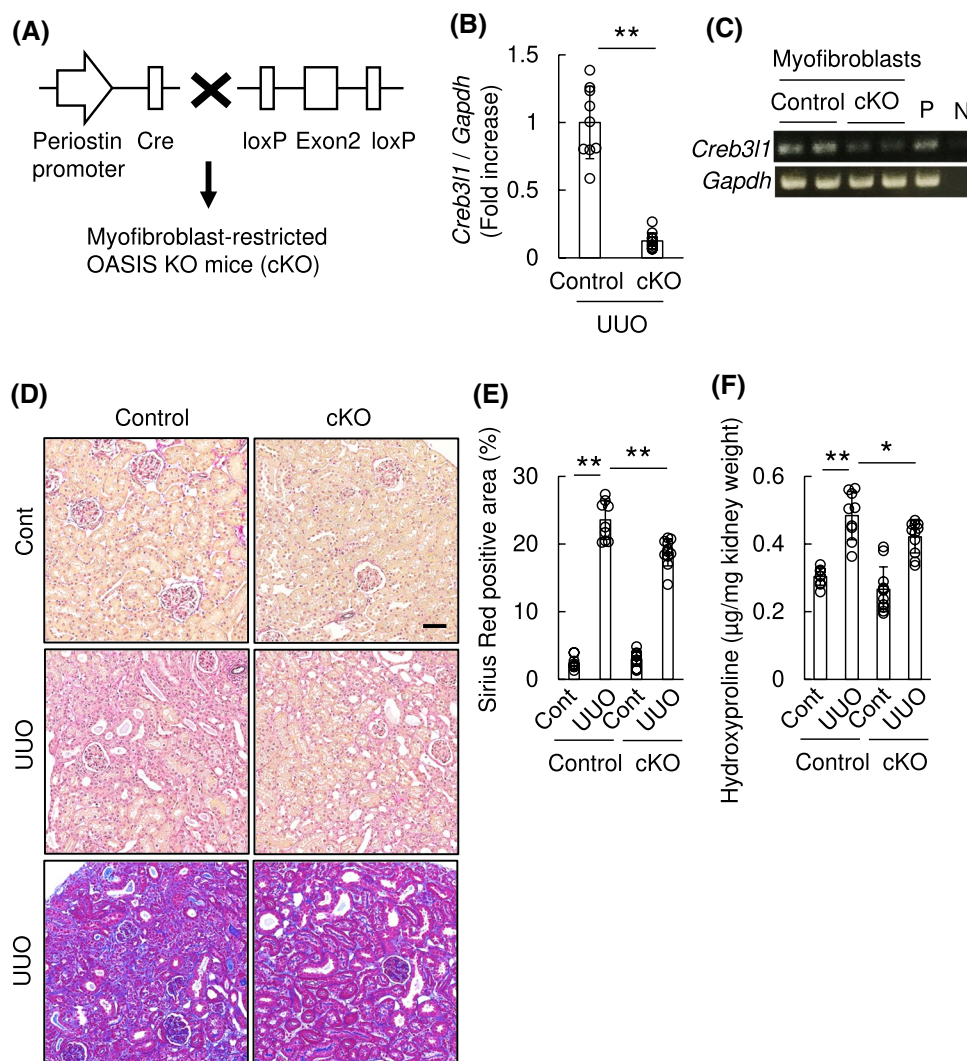


FIGURE 9 Myofibroblast-restricted *OASIS* deletion resulted in decreased kidney fibrosis after UUO. A, Generation of myofibroblasts-restricted *OASIS* KO (cKO) mice using Cre-loxP system. B, cKO and control mice were subjected to UUO. At Day 7 after UUO, quantitative PCR was performed for transcript expression of *OASIS/Creb311*. The expression of the transcripts was normalized to that of *Gapdh*. ** $P < .01$ by Student *t* test. C, Myofibroblasts were isolated from kidney of cKO and control. The transcript expression of *OASIS/Creb311* was examined by PCR. P: positive control, N: negative control. D, Sirius Red (upper and middle panel) or Masson's trichrome (lower panel) staining was performed. Representative images are shown. Bar: 50 μ m. E, Sirius Red positive area was measured. F, Hydroxyproline assay was performed. G, Immunofluorescence analysis was performed with anti-Ki-67 antibody, anti- α -SMA antibody and DAPI. Representative images are shown. Bar: 50 μ m. H and I, The number of α -SMA+ cells (H) and the number of Ki-67 + α -SMA+ cells (I) was quantitatively evaluated. J-O, Quantitative PCR was performed for transcript expression of *Tgfb1*, *Col 1*, *Col 3*, *Mmp2*, *Mmp9*, and *Bst2*. The expression of the transcripts was normalized to that of *Gapdh*. * $P < .05$, ** $P < .01$ by one-way ANOVA followed by Dunnett test. Data are shown as mean \pm SD (n = 9 for control, n = 11 for cKO)

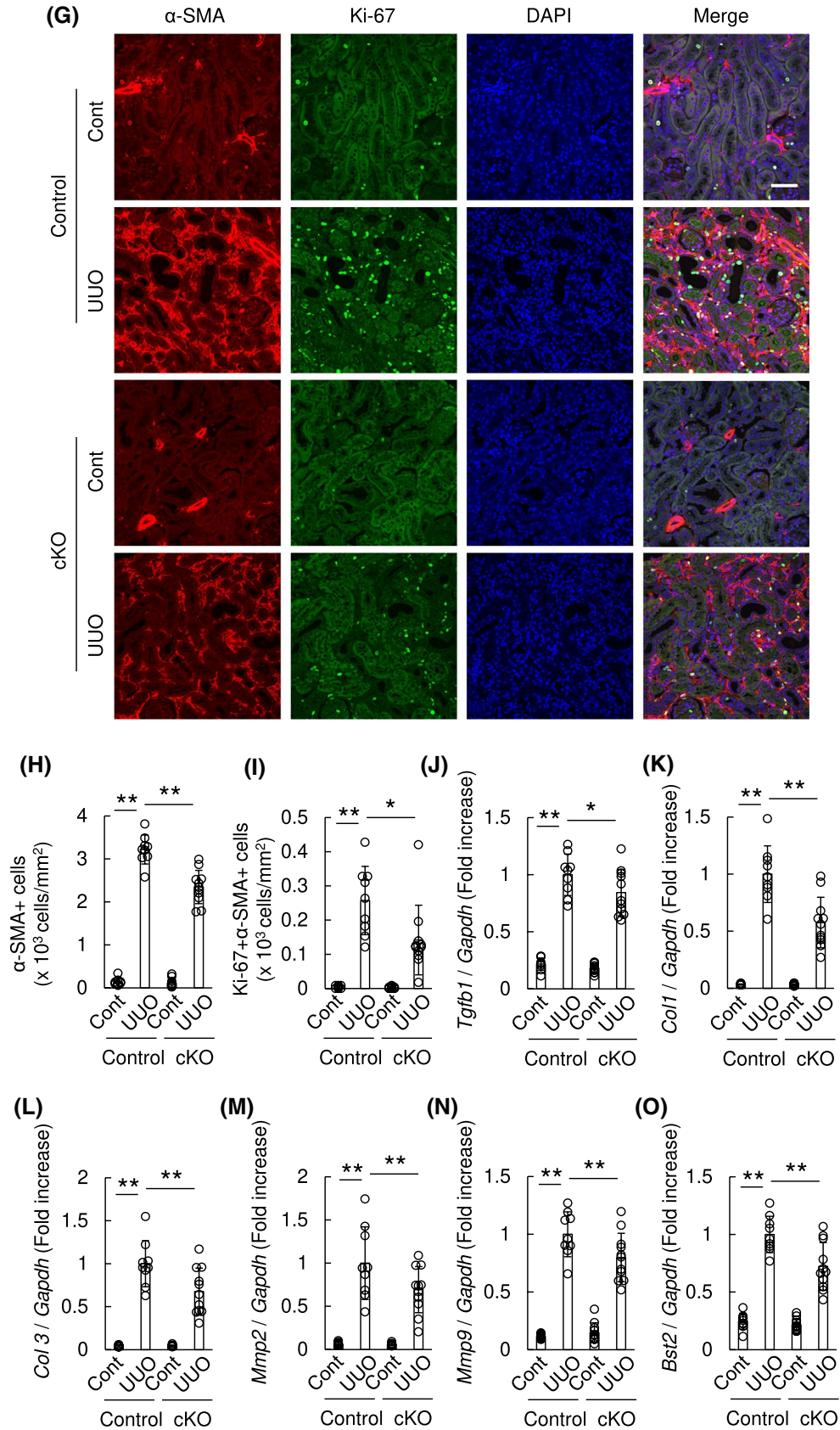
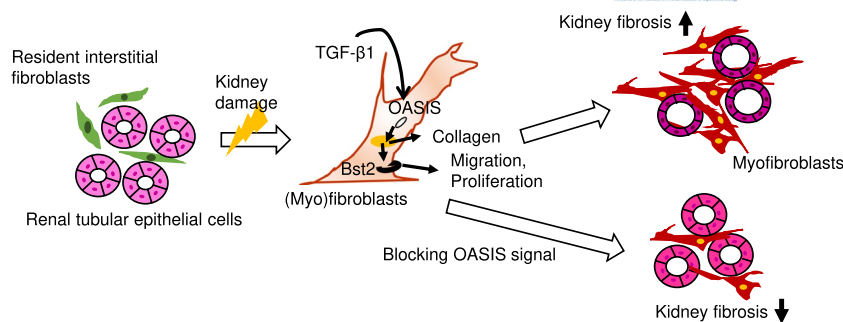


FIGURE 9 (Continued)

FIGURE 10 The graphical abstract of this study. OASIS is induced by TGF- β 1 and promotes collagen synthesis in myofibroblasts. Furthermore, OASIS contributes to progressive kidney fibrosis by facilitating migration and proliferation of myofibroblasts, accompanied by increased Bst2 expression



on 6 regions, designated as region 1-6. Chromatin immunoprecipitation revealed that OASIS directly bound to the upstream regions of the *Bst2* gene promoter, including region 2, 3, 5, and 6 (Figure 8D). Next, to discover whether Bst2 itself regulates kidney fibrosis, WT mice were subjected to UUO, followed by single treatment with anti-Bst2 monoclonal blocking antibody or non-immune IgG κ , as a control, at 100 μ g/body (Figure 8E-G). Although anti-Bst2 antibody is used for depletion of plasmacytoid dendritic cells (pDCs),³⁵ we confirmed that single injection of anti-Bst2 antibody at 100 μ g/body did not affect pDCs expression in both kidney and spleen after UUO (Figure S8). Histological analysis and hydroxyproline assays revealed that kidney fibrosis was significantly attenuated in the anti-Bst2 antibody-treated group compared with the control IgG κ -treated group (Sirius Red positive area: control IgG; $22.0 \pm 2.0\%$, anti-Bst2 antibody; $15.2 \pm 5.1\%$, hydroxyproline content: control IgG κ ; 0.60 ± 0.08 μ g/mg, anti-Bst2 antibody; 0.49 ± 0.09 μ g/mg). In addition, when *OASIS* KO mice were treated with anti-Bst2 antibody to examine whether Bst2 mediates the effects of OASIS during kidney fibrosis (Figure 8H), we found that blockade of Bst2 failed to exhibit any further suppression of fibrosis after UUO in *OASIS* KO mice. Collectively, these data strongly suggest that OASIS promotes kidney fibrosis, at least partly, by increased expression of Bst2.

3.7 | Myofibroblasts-restricted OASIS ablation resulted in resistance to kidney fibrosis

Finally, to determine the myofibroblast-specific requirement of OASIS in fibrotic kidneys, we generated myofibroblast-restricted *OASIS* conditional knockout (*OASIS* cKO) mice using myofibroblast *Postn* promoter-driven Cre-loxP recombination system (Figure 9A).²² First, it was confirmed that the *Postn* promoter drives Cre recombinase protein expression within cells in renal interstitial fibrotic areas and in glomeruli of *OASIS* cKO mice Day 7 after UUO (Figure S9), however, Cre protein is undetectable in WT kidneys. Moreover, the expression of *OASIS/Creb3l1* mRNA

was dramatically decreased in UUO-kidney and isolated myofibroblasts of *OASIS* cKO mice following Cre/loxP recombination (Figure 9B,C). These data indicate that, at least, *OASIS* deletion in myofibroblasts via *Postn-Cre* resulted in efficient suppression of *OASIS*. Intriguingly, *OASIS* cKO mice showed significantly reduced Sirius red and Masson's trichrome staining, hydroxyproline collagen content and number of α -SMA positive cells in kidneys after UUO, when compared with control (Figure 9D-H). Additionally, the number of Ki-67 positive myofibroblasts was decreased in kidneys of *OASIS* cKO mice after UUO compared with control (Figure 9G,I). The mRNA expression of *Tgfb1*, *Coll1*, *Col3*, *Mmp2*, *Mmp9*, and *Bst2* was significantly decreased in *OASIS* cKO mice (Figure 9J-O). Taken together, these data demonstrate that OASIS expression within the myofibroblast lineage contributes to the pathogenesis of kidney fibrosis.

4 | DISCUSSION

OASIS was originally identified as an ER stress transducer as it was upregulated in response to ER stress in astrocytes, leading to increased GRP78 expression, an ER stress-response indicator gene.⁶ However, OASIS does not uniformly function in every organ's ER-stress as it did not induce classical ER stress-response gene in pancreatic β -cells.³⁶ In this study, we demonstrate that in the fibrotic kidney, OASIS expression was unaffected by ER-stress inducer tunicamycin but was induced via TGF- β 1. Moreover, although a previous human lung carcinoma cell study showed that TGF- β 1 activated OASIS simply by proteolyzing its full-length form,²⁷ our data revealed that TGF- β 1 induced both the active and full-length forms of OASIS in renal myofibroblasts. Combined these data suggest that not only is TGF- β 1 an important inducer of active OASIS, but it is likely that OASIS signaling network is differentially regulated in an organ and maybe even cell type-dependent manner. In addition, unexpectedly, overexpression of active form of *OASIS/Creb3l1* reduced migration of (myo) fibroblasts as well as *OASIS/Creb3l1* knockdown with TGF- β 1 stimulation. Since it has reported that OASIS interacts with hypoxia-inducible factor-1 α ¹⁸ or Smad4,²⁷ we

speculate the roles of OASIS could not be explained by its expression level and OASIS exerts divergent functions depending on the pathological conditions.

The pro-fibrotic TGF- β pathway transmits its signals through Smad-dependent canonical and Smad-independent noncanonical pathways. Significantly, TGF- β 1 (the ligand used in our in vitro studies) is the predominant canonical effector of kidney fibrosis and is upregulated in response to UUO injury.³⁷ In addition, TGF- β 1 induces transformation of fibroblasts to myofibroblasts, which produce ECM proteins such as collagen fibers or fibronectin in the kidney interstitium.³⁸ Moreover, the Smad3 pathway has been shown to be essential for TGF- β 1-induced epithelial mesenchymal transition (EMT) and autoinduction of TGF- β 1. Thus, blocking TGF- β 1 and its downstream effectors can attenuate kidney injury and fibrosis.³⁷ Intriguingly, it has reported that Smad4, as a co-activator of OASIS, is required for OASIS-mediated induction of collagen.²⁷ In this study, we demonstrated that OASIS knockdown suppressed TGF- β 1-induced collagen1 α 1 expression in NRK49F cells and that OASIS bound the *Coll1a1* promoter in renal myofibroblasts. Moreover, although TGF- β was reported to activate human fibroblasts through non-Smad signaling,³⁹ OASIS did not influence TGF- β 1-mediated differentiation of fibroblast into myofibroblast. One possible reason why the expression of α -SMA, a myofibroblasts marker, was decreased in kidneys of OASIS KO mice and OASIS cKO mice after kidney injury is that the depletion of OASIS reduced the number of proliferative myofibroblasts. These data propose OASIS contributed to modification of myofibroblasts phenotype via TGF- β 1-mediated Smad-dependent canonical signaling, leading to reduced kidney fibrosis.

Qualitative changes within fibroblasts, with their increased migration capacity, is thought to be important to the progression pathology during lung fibrosis.⁴⁰ In this study, we identified profibrotic Bst2, a type II transmembrane glycoprotein,⁴¹ as an important potential downstream effector molecule of OASIS within kidney myofibroblasts. Bst2 is known as an antiviral protein that blocks the release of enveloped virus,^{42,43} but can regulate proliferation and cell migration in multiple tumors when overexpressed.^{31,32} Therefore, Bst2 is under investigation as a potential therapeutic target in cancer. However, to our knowledge, the significance of Bst2 in tissue fibrosis has not yet been described before. Significantly, we demonstrated that antibody blockade of Bst2 reduced kidney fibrosis and suggest the OASIS-Bst2 as a novel regulatory mechanism driving kidney fibrosis. In addition to Bst2, we have found that OASIS could modulate kidney fibrosis by regulating other fibrosis-related genes (see Figure 8A), particularly those genes reported to be associated with cell migration. For instance, in response to OASIS knockout, podoplanin (Pdpn) which promotes the human fibroblast migration was

identified.⁴⁴ Interestingly, growth differentiation factor-15 (GDF15), which is protective during acute kidney injury by its anti-inflammatory activity,⁴⁵ was upregulated in the OASIS-deleted myofibroblasts. Similarly, the expression of macrophage markers, such as CD11b and F4/80, and inflammatory cytokines, such as TNF- α , IL-1 β , and IL-6, was analyzed and found to be unchanged between WT and OASIS KO mice at Day 7 after UUO (data not shown), suggesting that OASIS gene ablation is unlikely to influence inflammatory reaction. This is important as the TGF- β 1 cytokine is also known to be released via infiltrating circulating pro-inflammatory cells, including macrophages.⁴⁶ Of course, we consider that OASIS-induced collagen synthesis is one possible mechanisms of the progression of kidney fibrosis. Taken together with results and observations, suppression of OASIS could attenuate kidney fibrosis through modifying the myofibroblast phenotype, via modulating multiple pro- and anti-fibrotic pathways, including pro-fibrotic Bst2. However, further studies are needed to determine the functional roles of Bst2 in kidney fibrosis and identification of its pro-fibrotic targets.

OASIS is cleaved by S1P/S2P, resulting in the release of the active domains which regulate the transcription of target genes. Since 4-(2-aminoethyl) benzenesulfonyl fluoride hydrochloride (AEBSF) inhibits site 1 protease irreversibly, leading to the suppression of OASIS activation,^{10,47,48} we examined whether pharmacological inhibition of OASIS by AEBSF reduced kidney fibrosis. Intriguingly, pre- and post-treatment with AEBSF significantly reduced kidney fibrosis after UUO (data not shown), indicating that OASIS could be a therapeutic target for fibrotic kidney diseases. However, AEBSF is a non-specific drug for OASIS since ATF 6 and SREBP-2 were also reported to be cleaved by S1P/S2P.⁴⁹⁻⁵¹ In fact, we confirmed the expression of ATF6 and SREBP-2 in NRK49F cells was decreased, to a lesser extent, after AEBSF treatment (data not shown). Additionally, deficiency of OASIS is linked to osteogenesis imperfecta in humans and mice.^{12,18,19} Therefore, we need to develop the agent to inhibit OASIS specifically, such as antisense oligonucleotides targeting OASIS, and the drug delivery method targeted to the tubulointerstitium in kidney in future research.

Limitation: There is some limitation in this study. First, although OASIS/*Creb3l1* mRNA was upregulated in kidneys after UUO, an increased protein expression of full-length of OASIS was not observed with a statistically significant difference because the protein expression of full-length of OASIS may be hard to detect in in vivo kidney samples with the antibody used in the experiments. Full-length form of OASIS is cleaved by S1P/S2P. S1P is reported to be activated by ER stress that is induced by UUO.^{52,53} Therefore, it is also likely that full-length of OASIS is immediately cleaved by S1P/S2P in murine UUO kidneys. Moreover, we could not clearly indicate the OASIS and α -SMA

expression in kidney by co-immunofluorescence because OASIS protein in kidney sections could not be specifically detected. Thus, we used immunohistochemical staining using an avidin-biotin-peroxidase and alkaline phosphatase detection system to identify OASIS and α -SMA expressed cells respectively. Furthermore, OASIS was broadly expressed in tubular epithelial cells in normal parts of human kidney, whereas OASIS was not clearly detected in tubular epithelial cells of normal murine kidney. Thus, there might be a difference in the expression pattern of OASIS in tubules between human kidney and murine kidney. In injured murine kidney, consistent with the data from *in situ* hybridization, OASIS protein was observed not only in myofibroblasts but also in injured tubular cells. OASIS protein staining intensity within α -SMA+ cells in the tubulointerstitium was higher compared to other area in both fibrotic human and fibrotic murine kidney. Additionally, using genetically modified mice, we have successfully demonstrated that OASIS is expressed in myofibroblasts. Therefore, we mainly focused on the roles of OASIS in myofibroblast, especially derived from fibroblasts, in *in vitro* assay. Although tubule cells also differentiated into myofibroblasts in diseased kidney,⁵⁴ the contribution of OASIS in the dilated tubules to the development of kidney fibrosis could not be identified. By the way, we confirmed TGF- β 1 could not induced OASIS expression in human proximal tubule (HK-2) cells (data not shown). Further studies are required to confirm the roles of OASIS in tubular epithelial cells and the origin of OASIS-positive myofibroblasts.

In conclusion, OASIS contributes to progressive kidney fibrosis by facilitating migration and proliferation of myofibroblasts, accompanied by increased Bst2 expression. Thus, the OASIS-Bst2 signaling axis is a novel mechanism responsible for the development of fibrotic kidney disease and may represent a useful therapeutic target to alleviate and/or prevent kidney fibrosis. Our findings provide the first evidence of the role of OASIS in kidney and during pathological responses to injury.

ACKNOWLEDGMENTS

We thank Hiroyuki Nakayama for his precious advice and Reiko Kizaki for her excellent administrative work. This study was supported by Center for Medical Research and Education, Graduate School of Medicine, Osaka University. This study was partially supported by MEXT/JSPS KAKENHI Grants 18K15027 to MO, and 18H02603 & 18K19545 to YF, as well as NIH R01 HL148165 Grant to SJC This study was also partially supported by Takeda Science Foundation to MO, Japanese Association of Dialysis Physicians to MO and Platform Project for Supporting Drug Discovery and Life Science Research (Basis for Supporting Innovative Drug Discovery and Life

Science Research (BINDS)) from AMED under Grant Number JP20am0101084.

CONFLICT OF INTEREST

The authors have declared that no conflict of interest exists.

AUTHOR CONTRIBUTIONS

Y. Fujio, and M. Obana designing research studies; A. Yamamoto, H. Morioki, T. Nakae, T. Harada, S. Noda, K. Matsumoto, M. Tomimatsu, and M. Obana conducting experiments; A. Yamamoto, H. Morioki, T. Nakae, T. Harada, and M. Obana acquiring data; A. Yamamoto, Y. Miyake, T. Harada, S. Mitsuoka, K. Matsumoto, S. Tanaka, and M. Maeda analyzing data; S. Kanemoto, S.J. Conway, and K. Imaizumi providing reagents; A. Yamamoto, S.J. Conway, Y. Fujio, and M. Obana, writing the manuscript.

REFERENCES

1. Go AS, Chertow GM, Fan D, McCulloch CE, Hsu CY. Chronic kidney disease and the risks of death, cardiovascular events, and hospitalization. *N Engl J Med*. 2004;351(13):1296-1305.
2. Keith DS, Nichols GA, Gullion CM, Brown JB, Smith DH. Longitudinal follow-up and outcomes among a population with chronic kidney disease in a large managed care organization. *Arch Intern Med*. 2004;164(6):659-663.
3. Moll S, Meier M, Formentini I, Pomposiello S, Prunotto M. New renal drug development to face chronic renal disease. *Expert Opin Drug Discov*. 2014;9(12):1471-1485.
4. Farris AB, Colvin RB. Renal interstitial fibrosis: mechanisms and evaluation. *Curr Opin Nephrol Hypertens*. 2012;21(3):289-300.
5. Strutz F, Zeisberg M. Renal fibroblasts and myofibroblasts in chronic kidney disease. *J Am Soc Nephrol*. 2006;17(11):2992-2998.
6. Kondo S, Murakami T, Tatsumi K, et al. OASIS, a CREB/ATF-family member, modulates UPR signalling in astrocytes. *Nat Cell Biol*. 2005;7(2):186-194.
7. Kondo S, Saito A, Hino S-I, et al. BBF2H7, a novel transmembrane bZIP transcription factor, is a new type of endoplasmic reticulum stress transducer. *Mol Cell Biol*. 2007;27(5):1716-1729.
8. Asada R, Kanemoto S, Kondo S, Saito A, Imaizumi K. The signalling from endoplasmic reticulum-resident bZIP transcription factors involved in diverse cellular physiology. *J Biochem*. 2011;149(5):507-518.
9. Kanemoto S, Kobayashi Y, Yamashita T, et al. Luman is involved in osteoclastogenesis through the regulation of DC-STAMP expression, stability and localization. *J Cell Sci*. 2015;128(23):4353-4365.
10. Murakami T, Kondo S, Ogata M, et al. Cleavage of the membrane-bound transcription factor OASIS in response to endoplasmic reticulum stress. *J Neurochem*. 2006;96(4):1090-1100.
11. Vellanki RN, Zhang L, Volchuk A. OASIS/CREB3L1 is induced by endoplasmic reticulum stress in human glioma cell lines and contributes to the unfolded protein response, extracellular matrix production and cell migration. *PLoS ONE*. 2013;8(1):e54060.
12. Murakami T, Saito A, Hino S-I, et al. Signalling mediated by the endoplasmic reticulum stress transducer OASIS is involved in bone formation. *Nat Cell Biol*. 2009;11(10):1205-1211.

13. Zhu H-Y, Bai W-D, Liu J-Q, et al. Up-regulation of FGFBP1 signaling contributes to miR-146a-induced angiogenesis in human umbilical vein endothelial cells. *Sci Rep*. 2016;6:25272.
14. Mellor P, Deibert L, Calvert B, Bonham K, Carlsen SA, Anderson DH. CREB3L1 is a metastasis suppressor that represses expression of genes regulating metastasis, invasion, and angiogenesis. *Mol Cell Biol*. 2013;33(24):4985-4995.
15. Rose M, Schubert C, Dierichs L, et al. OASIS/CREB3L1 is epigenetically silenced in human bladder cancer facilitating tumor cell spreading and migration in vitro. *Epigenetics*. 2014;9(12):1626-1640.
16. Ward AK, Mellor P, Smith SE, et al. Epigenetic silencing of CREB3L1 by DNA methylation is associated with high-grade metastatic breast cancers with poor prognosis and is prevalent in triple negative breast cancers. *Breast Cancer Res*. 2016;18(1):12.
17. Hino K, Saito A, Asada R, Kanemoto S, Imaizumi K. Increased susceptibility to dextran sulfate sodium-induced colitis in the endoplasmic reticulum stress transducer OASIS deficient mice. *PLoS ONE*. 2014;9(2):e88048.
18. Cui M, Kanemoto S, Cui X, et al. OASIS modulates hypoxia pathway activity to regulate bone angiogenesis. *Sci Rep*. 2015;5:16455.
19. Lindahl K, Åström E, Dragomir A, et al. Homozygosity for CREB3L1 premature stop codon in first case of recessive osteogenesis imperfecta associated with OASIS-deficiency to survive infancy. *Bone*. 2018;114:268-277.
20. Conway SJ, Izuhara K, Kudo Y, et al. The role of periostin in tissue remodeling across health and disease. *Cell Mol Life Sci*. 2014;71(7):1279-1288.
21. Kramann R, Fleig SV, Schneider RK, et al. Pharmacological GLI2 inhibition prevents myofibroblast cell-cycle progression and reduces kidney fibrosis. *J Clin Invest*. 2015;125(8):2935-2951.
22. Imaeda A, Tanaka S, Tonegawa K, et al. Myofibroblast beta2 adrenergic signaling amplifies cardiac hypertrophy in mice. *Biochem Biophys Res Commun*. 2019;510(1):149-155.
23. Fu P, Liu F, Su S, et al. Signaling mechanism of renal fibrosis in unilateral ureteral obstructive kidney disease in ROCK1 knockout mice. *J Am Soc Nephrol*. 2006;17(11):3105-3114.
24. Kanno Y, Kawashita E, Kokado A, et al. alpha2AP mediated myofibroblast formation and the development of renal fibrosis in unilateral ureteral obstruction. *Sci Rep*. 2014;4:5967.
25. Obana M, Maeda M, Takeda K, et al. Therapeutic activation of signal transducer and activator of transcription 3 by interleukin-11 ameliorates cardiac fibrosis after myocardial infarction. *Circulation*. 2010;121(5):684-691.
26. Asada N, Takase M, Nakamura J, et al. Dysfunction of fibroblasts of extrarenal origin underlies renal fibrosis and renal anemia in mice. *J Clin Invest*. 2011;121(10):3981-3990.
27. Chen Q, Lee CE, Denard B, Ye J. Sustained induction of collagen synthesis by TGF-beta requires regulated intramembrane proteolysis of CREB3L1. *PLoS ONE*. 2014;9(10):e108528.
28. Di J, Jiang L, Zhou Y, et al. Ets-1 targeted by microRNA-221 regulates angiotensin II-induced renal fibroblast activation and fibrosis. *Cell Physiol Biochem*. 2014;34(4):1063-1074.
29. Wang H, Qian J, Zhao X, Xing C, Sun B. beta-Aminoisobutyric acid ameliorates the renal fibrosis in mouse obstructed kidneys via inhibition of renal fibroblast activation and fibrosis. *J Pharmacol Sci*. 2017;133(4):203-213.
30. Rosenkranz S. TGF-beta1 and angiotensin networking in cardiac remodeling. *Cardiovasc Res*. 2004;63(3):423-432.
31. Gu G, Zhao D, Yin Z, Liu P. BST-2 binding with cellular MT1-MMP blocks cell growth and migration via decreasing MMP2 activity. *J Cell Biochem*. 2012;113(3):1013-1021.
32. Liu W, Cao Y, Guan Y, Zheng C. BST2 promotes cell proliferation, migration and induces NF-kappaB activation in gastric cancer. *Biotechnol Lett*. 2018;40(7):1015-1027.
33. Bego MG, Mercier J, Cohen EA. Virus-activated interferon regulatory factor 7 upregulates expression of the interferon-regulated BST2 gene independently of interferon signaling. *J Virol*. 2012;86(7):3513-3527.
34. Deng H, Guan X, Gong L, et al. CBX6 is negatively regulated by EZH2 and plays a potential tumor suppressor role in breast cancer. *Sci Rep*. 2019;9(1):197.
35. Goubier A, Dubois B, Gheit H, et al. Plasmacytoid dendritic cells mediate oral tolerance. *Immunity*. 2008;29(3):464-475.
36. Vellanki RN, Zhang L, Guney MA, Rocheleau JV, Gannon M, Volchuk A. OASIS/CREB3L1 induces expression of genes involved in extracellular matrix production but not classical endoplasmic reticulum stress response genes in pancreatic beta-cells. *Endocrinology*. 2010;151(9):4146-4157.
37. Sato M, Muragaki Y, Saika S, Roberts AB, Ooshima A. Targeted disruption of TGF-beta1/Smad3 signaling protects against renal tubulointerstitial fibrosis induced by unilateral ureteral obstruction. *J Clin Invest*. 2003;112(10):1486-1494.
38. Wu CF, Chiang WC, Lai CF, et al. Transforming growth factor beta-1 stimulates profibrotic epithelial signaling to activate pericyte-myofibroblast transition in obstructive kidney fibrosis. *Am J Pathol*. 2013;182(1):118-131.
39. Carthy JM, Sundqvist A, Heldin A, et al. Tamoxifen inhibits TGF-beta-mediated activation of myofibroblasts by blocking non-smad signaling through ERK1/2. *J Cell Physiol*. 2015;230(12):3084-3092.
40. Tsukui T, Ueha S, Abe J, et al. Qualitative rather than quantitative changes are hallmarks of fibroblasts in bleomycin-induced pulmonary fibrosis. *Am J Pathol*. 2013;183(3):758-773.
41. Goto T, Kennel SJ, Abe M, et al. A novel membrane antigen selectively expressed on terminally differentiated human B cells. *Blood*. 1994;84(6):1922-1930.
42. Neil SJ, Zang T, Bieniasz PD. Tetherin inhibits retrovirus release and is antagonized by HIV-1 Vpu. *Nature*. 2008;451(7177):425-430.
43. Jouvenet N, Neil SJD, Zhadina M, et al. Broad-spectrum inhibition of retroviral and filoviral particle release by tetherin. *J Virol*. 2009;83(4):1837-1844.
44. Suchanski J, Tejchman A, Zacharski M, et al. Podoplanin increases the migration of human fibroblasts and affects the endothelial cell network formation: A possible role for cancer-associated fibroblasts in breast cancer progression. *PLoS ONE*. 2017;12(9):e0184970.
45. Abulizi P, Loganathan N, Zhao D, et al. Growth differentiation factor-15 deficiency augments inflammatory response and exacerbates septic heart and renal injury induced by lipopolysaccharide. *Sci Rep*. 2017;7(1):1037.
46. Liu Y. Cellular and molecular mechanisms of renal fibrosis. *Nat Rev Nephrol*. 2011;7(12):684-696.
47. Gorski JP, Huffman NT, Chittur S, et al. Inhibition of proprotein convertase SKI-1 blocks transcription of key extracellular matrix genes regulating osteoblastic mineralization. *J Biol Chem*. 2011;286(3):1836-1849.
48. Feng YX, Jin DX, Sokol ES, Reinhardt F, Miller DH, Gupta PB. Cancer-specific PERK signaling drives invasion and metastasis through CREB3L1. *Nat Commun*. 2017;8(1):1079.

49. Ye J, Rawson RB, Komuro R, et al. ER stress induces cleavage of membrane-bound ATF6 by the same proteases that process SREBPs. *Mol Cell*. 2000;6(6):1355-1364.
50. Shen J, Chen X, Hendershot L, Prywes R. ER stress regulation of ATF6 localization by dissociation of BiP/GRP78 binding and unmasking of Golgi localization signals. *Dev Cell*. 2002;3(1):99-111.
51. Okada T, Haze K, Nakanaka S, et al. A serine protease inhibitor prevents endoplasmic reticulum stress-induced cleavage but not transport of the membrane-bound transcription factor ATF6. *J Biol Chem*. 2003;278(33):31024-31032.
52. Kim JY, Garcia-Carbonell R, Yamachika S, et al. ER stress drives lipogenesis and steatohepatitis via caspase-2 activation of S1P. *Cell*. 2018;175(1):133-145 e115.
53. Chiang C-K, Hsu S-P, Wu C-T, et al. Endoplasmic reticulum stress implicated in the development of renal fibrosis. *Mol Med*. 2011;17(11-12):1295-1305.
54. Eddy AA. The origin of scar-forming kidney myofibroblasts. *Nat Med*. 2013;19(8):964-966.

SUPPORTING INFORMATION

Additional Supporting Information may be found online in the Supporting Information section.

How to cite this article: Yamamoto A, Morioki H, Nakae T, et al. Transcription factor old astrocyte specifically induced substance is a novel regulator of kidney fibrosis. *The FASEB Journal*. 2021;35:e21158. <https://doi.org/10.1096/fj.202001820R>